Click Here for Full Article

NO$_x$ emission trends for China, 1995–2004: The view from the ground and the view from space

Qiang Zhang,[1] David G. Streets,[1] Kebin He,[2] Yuxuan Wang,[3] Andreas Richter,[4] John P. Burrows,[4] Itsushi Uno,[5] Carey J. Jang,[6] Dan Chen,[2] Zhiliang Yao,[2] and Yu Lei[2]

[1] A rapid increase of NO$_2$ columns over China has been observed by satellite instruments in recent years. We present a 10-a regional trend of NO$_x$ emissions in China from 1995 to 2004 using a bottom-up methodology and compare the emission trends with the NO$_2$ column trends observed from GOME and SCIAMACHY, the two spaceborne instruments. We use a dynamic methodology to reflect the dramatic change in China's NO$_x$ emissions caused by energy growth and technology renewal. We use a scenario analysis approach to identify the possible sources of uncertainties in the current bottom-up inventory, in comparison with the satellite observation data. Our best estimates for China's NO$_x$ emissions are 10.9 Tg in 1995 and 18.6 Tg in 2004, increasing by 70% during the period considered. NO$_x$ emissions and satellite-based NO$_2$ columns show broad agreement in temporal evolution and spatial distribution. Both the emission inventory data and the satellite observations indicate a continuous and accelerating growth rate between 1996 and 2004 over east central China. However, the growth rate from the emission inventory is lower than that from the satellite observations. From 1996 to 2004, NO$_x$ emissions over the region increased by 61% according to the inventory, while a 95% increase in the NO$_2$ columns measured by satellite was observed during the same period. We found good agreement during summertime but a large discrepancy during wintertime. The consistency between the summertime trends suggests that the bias cannot be due to systematic error of activity data or emission factors. The reasons for the discrepancy cannot yet be fully identified, but possible explanations include an underestimation in seasonal emission variations, variability of meteorology, NO$_x$ injection height, and the increasing trend of sulfate aerosols.

Citation: Zhang, Q., et al. (2007), NO$_x$ emission trends for China, 1995–2004: The view from the ground and the view from space, *J. Geophys. Res.*, *112*, D22306, doi:10.1029/2007JD008684.

1. Introduction

[2] Nitrogen oxides (NO$_x$ ≡ NO + NO$_2$) play a key role in tropospheric chemistry. Production of ozone in the troposphere is controlled by the abundance of NO$_x$. Anthropogenic activity has increased global NO$_x$ emissions by a factor of 3–6 since preindustrial times [*Prather et al.*, 2001], and China is thought to contribute more than 10% of present-day global anthropogenic NO$_x$ emissions [*Olivier et al.*, 1996, 1999]. Moreover, global NO$_x$ emissions are expected to increase by more than 50% during the period 2000–2020 [*Intergovernmental Panel on Climate Change*, 2001], with most of the increase coming from Asia.

[3] Up to now, developing an understanding of China's NO$_x$ emissions has largely relied on bottom-up approaches that aggregate fuel combustion data and emission factors. The first bottom-up inventory of China's NO$_x$ emissions was developed by *Kato and Akimoto* [1992] and *Akimoto and Narita* [1994] for late-1980s emissions. After that, several bottom-up studies were conducted to estimate China's NO$_x$ emissions in the period 1990–1995, as part of China's national inventory or as part of regional/global inventories [*Bai*, 1996; *Wang et al.*, 1996; *Olivier et al.*, 1998, 1999; *van Aardenne et al.*, 1999; *Xue et al.*, 1999; *Shah et al.*, 2000; *Streets and Waldhoff*, 2000; *Klimont et al.*, 2001; *Streets et al.*, 2001; *Vallack et al.*, 2001]. All these studies estimated emissions for a single year rather than an emission trend, although a few studies also presented emission projections [*van Aardenne et al.*, 1999; *Shah et al.*, 2000; *Klimont et al.*, 2001]. The year 1995 was a focus

[1]Decision and Information Sciences Division, Argonne National Laboratory, Argonne, Illinois, USA.
[2]Department of Environmental Science and Engineering, Tsinghua University, Beijing, China.
[3]Division of Engineering and Applied Sciences and Department of Earth and Planetary Sciences, Harvard University, Cambridge, Massachusetts, USA.
[4]Institute of Environmental Physics, University of Bremen, Bremen, Germany.
[5]Research Institute for Applied Mechanics, Kyushu University, Fukuoka, Japan.
[6]Office of Air Quality Planning and Standards, U.S. Environmental Protection Agency, Research Triangle Park, North Carolina, USA.

Table 1. Estimates of China's Annual NO$_x$ Emissions[a]

	Sources	Region	1995	1996	1997	1998	1999	2000	2001	2002	2003	2004
Emission inventory methods												
Xue et al. [1999]	FF	China	3.2									
Streets and Waldhoff [2000]	FF + BF + BB	China	3.6									
Klimont et al. [2001]	FF + BF	China	3.0									
Streets et al. [2001]	FF + BF	China	3.4	3.7	3.8							
Vallack et al. [2001]	FF + BF	China	4.0									
Hao et al. [2002]	FF	China	3.4	3.7	3.6	3.4						
Streets et al. [2003]	FF + BF	China						3.2				
Olivier et al. [2005]	FF + BF	China	3.7					4.2				
This study	FF + BF	China	3.3	3.5	3.5	3.6	3.7	3.8	4.0	4.4	4.9	5.7
Inverse modeling methods												
Martin et al. [2003]	all	east Asia			4.7							
Wang et al. [2004]	FF + BF	China							5.0			
Jaeglé et al. [2005]	FF + BF	China						4.4				
Martin et al. [2006]	all	east Asia										9.8
Wang et al. [2007]	FF + BF	east China			3.7							

[a]Units are Tg-N/a. FF, fossil fuel; BF, biofuel combustion; BB, open biomass burning; and all, FF + BF + BB + soil emissions.

year of many of the above studies. The range of 1995 emission estimates is from 9.7 Tg to 13.1 Tg, with the lowest estimates being by *Klimont et al.* [2001] and the highest by *Vallack et al.* [2001]. *Hao et al.* [2002] and *Tian* [2003] were the first to present estimates of the trend in China's NO$_x$ emissions during the 1990s. Their work showed an increasing trend for the early 1990s and a decreasing trend after the year 1996, due to a decrease in coal consumption. The most recent NO$_x$ emission inventory for China is given by *Streets et al.* [2003], as part of the NASA TRACE-P inventory. They estimated China's NO$_x$ emissions in 2000 to be 11.3 Tg, slightly lower than their previous estimates [*Streets and Waldhoff*, 2000; *Streets et al.*, 2001].

[4] China's emission inventories are thought to be quite uncertain, because of the lack of accurate statistics and emission factors. However, early NO$_x$ inventories for China were rarely examined in a comprehensive way, because of the lack of observational data. *Wang et al.* [2004] evaluated China's TRACE-P NO$_x$ emissions [*Streets et al.*, 2003] using ground station and aircraft observations during the TRACE-P field campaign and required a 47% increase of China's NO$_x$ emissions to obtain good agreement. This is rather similar to the situation with China's CO emissions, in which a postmission synthesis of TRACE-P measurements, inverse modeling, and MOPITT satellite retrievals led to a 36% increase in the estimate of China's CO emissions [*Streets et al.*, 2006]. Recent developments in space-based observations of NO$_2$ columns provide important new resources for evaluating emission inventories. The reanalysis of NO$_2$ columns inferred from the Global Ozone Monitoring Experiment (GOME) instrument [*Burrows et al.*, 1999] and the Scanning Imaging Absorption Spectrometer for Atmospheric Chartography (SCIAMACHY) instrument [*Bovensman et al.*, 1999] shows great potential for improving emission inventories at global and regional scale; and recent studies show good agreement with bottom-up inventories in industrialized regions of North America and Europe, where the confidence in emission inventories is high [*Beirle et al.*, 2003; *Martin et al.*, 2003, 2006; *Jaeglé et al.*, 2005; *Richter et al.*, 2005; *Kim et al.*, 2006; *van Noije et al.*, 2006]. These recent studies using space-based observations raise questions about the accuracy of China's NO$_x$ inventory.

2. Accuracy of NO$_x$ Emission Estimates for China

[5] Table 1 summarizes estimates of annual NO$_x$ emissions in China for the time period of this present study that have been obtained by bottom-up inventory methods and inverse modeling. The issues concerning China's NO$_x$ emissions that have been raised by inverse modeling studies focus on two aspects:

2.1. Accuracy of the Magnitude of Emissions and Their Seasonal Variations

[6] Several inverse modeling analyses constrained by space-based observational data have been conducted to estimate global or regional NO$_x$ emissions using the GEOS-Chem three-dimensional global chemical transport model. These studies used the standard NO$_x$ emission inventory in the GEOS-Chem model as the a priori, which were from the Global Emission Inventory Activity (GEIA) data set [*Benkovitz et al.*, 1996], and scaled emissions to the year 1998 [*Bey et al.*, 2001]. *Martin et al.* [2003] used GOME NO$_2$ columns for 1996–1997 and the GEOS-Chem model to estimate that the total NO$_x$ emissions in east Asia were 4.7 Tg N/a, in good agreement with the a priori value. Recently, this group performed a similar study but used SCIAMACHY NO$_2$ data of 2004–2005 [*Martin et al.*, 2006]. In this work they suggested that a posteriori emissions for east Asia were 9.8 Tg N/a, 46% higher than their a priori value of 6.7 Tg N/a. Because the a priori inventory they used was for the year 1998, the difference may reflect emissions growth in recent years. *Jaeglé et al.* [2005] also used GOME data and the GEOS-Chem model to invert global NO$_x$ emissions and provide top-down estimates for emissions from combustion sources, biomass burning, and soil sources, separately. Their a posteriori NO$_x$ emission estimate for combustion sources in China was 4.4 Tg N/a for the year 2000, 38% higher than the *Streets et al.* [2003] inventory. Subsequently, *Wang et al.* [2007] used a similar methodology but focused on the seasonal variability of NO$_x$ sources over the east China region. They used the same inventory as *Martin et al.* [2006] as the a priori, and estimated the a posteriori values of total NO$_x$ emissions and combustion NO$_x$ emissions for east China to be 4.7 Tg N/a and 3.5 Tg N/a, 33% and 8% higher than the a priori, respectively. Other researchers have performed forward

modeling studies and compared their results with satellite NO$_2$ columns over China [*Ma et al.*, 2006; *Uno et al.*, 2007; *He et al.*, 2007]. The modeled NO$_2$ columns underestimated the satellite retrievals by more than a factor of two over east China. These researchers also tended to attribute the difference to underestimation of emissions, but they did not quantify the ratio of observed to inventory emissions.

[7] The strong seasonality of NO$_x$ emissions in China has also been examined in satellite-based studies. *Jaeglé et al.* [2005] suggested that the ratio of monthly emissions in December (maximum) to emissions in July (minimum) is 1.4 in east Asia, higher than the value of 1.2 presented by *Streets et al.* [2003]. Finally, *Wang et al.* [2007] suggested that the a posteriori inventory for combustion sources for north China is 45% higher than the a priori value in winter, while the difference is only a few percent for other seasons, suggesting that the seasonality profiles in current inventories might be inappropriate.

2.2. Shape of Emission Trends Over the Past Decade

[8] A dramatic increase in NO$_2$ emissions over China is revealed by inspection of the GOME and SCIAMACHY satellite retrievals. *Richter et al.* [2005] were the first to reveal significant trends for NO$_2$ columns over east central China (ECC) during the period 1996–2002, which they attributed to increases in local emissions. They found a steady increase in NO$_2$ columns during this period, with accelerated growth during recent years. *Irie et al.* [2005] evaluated GOME NO$_2$ columns for this period and compared them with NO$_2$ columns from ground-based UV/visible spectrometers at clean sites, lending support to the results of *Richter et al.* [2005]. Subsequently, *van der A et al.* [2006] presented NO$_2$ column trends over China for the period 1996–2005 on a 1° × 1° grid. Their results also showed large growth in NO$_2$ column retrievals over east China.

[9] Previous inventory studies have clearly shown NO$_x$ emissions growth in the early 1990s but suggest a decreasing or flat trend during 1995–2000 [*Streets and Waldhoff*, 2000; *Streets et al.*, 2003; *Hao et al.*, 2002]; this is not supported by the view from space. After 2000, there have been no inventory trends reported. A systematic compilation of bottom-up NO$_x$ emission trends for China throughout the 1995–2005 period is absent. The purpose of this paper is to remedy that situation by developing a new, comprehensive view of China's NO$_x$ emission trends using bottom-up methods, and to compare it with the satellite-based trends to see if the view from space is a reasonable reflection of local emission trends.

3. A Dynamic Methodology for Emissions Estimation

[10] Building a long time series of emissions for China is more difficult than calculating emissions for a single year. Activity rates can change dramatically over just a few years, and net emission factors can also change. In a rapidly developing country like China, new technologies are constantly coming into the marketplace, sometimes to replace older technologies, sometimes not, causing rapid changes in net emission rates. Therefore, to build a reliable picture of

emission trends, it is necessary to develop a representation of the dynamic change driven by the technology renewal process, rather than simply to use year-by-year activity data with fixed emission factors.

[11] In this work, we use a dynamic methodology to reflect the change in China's NO$_x$ emissions over the 10-a period 1995–2004. We have carefully examined the technology renewal progress in the past 10 a in China, and identified three types of new technology that might have a strong influence on China's NO$_x$ emission trend: (1) low-NO$_x$ burner technology (LNB) in power plants, (2) the so-called "new-dry" process kilns in the cement industry, and (3) vehicle emission control technologies. We use different approaches to represent the penetration of those new technologies over time.

[12] Availability, consistency, and accuracy of data are other serious limitations to establishing reliable long-term emission trends. We relied for a large part of this work on government statistics. However, when we reviewed the available data sets in China for the 10-a period, a number of problems were apparent: lack of detailed activity data, breaks in time series, and inconsistency among different data sources, some of which have previously been noted by other researchers [*Sinton and Fridley*, 2000; *Sinton*, 2001; *Akimoto et al.*, 2006]. Clearly, those deficiencies increase the uncertainty of the emission estimates and, more seriously, can lead to different types of trends. In this work, we first generate the best guess emission scenario (BGE) that reflects our current best understanding of China's situation. However, because of the problems outlined above, it is difficult to guarantee that this scenario represents the actual NO$_x$ emission trend in China. Therefore, in order to analyze the sensitivities of assumptions and to quantify the emission uncertainties, we present a series of alternative emission scenarios based on our dynamic methodology. The assumptions of these scenarios encompass the ranges of possible variations of activity rates and emission factors, and thus the results reflect different aspects of the possible pathways of future NO$_x$ emissions in China.

[13] We have implemented an improved, technology-based methodology to build a 10-a regional trend of NO$_x$ emissions in China. The approach used in this work has been described in *Streets et al.* [2006], in connection with the development of an improved CO emission inventory for China. In this new emission model, we first classify anthropogenic NO$_x$ emission sources into two groups: stationary combustion and mobile source emissions. Then, for a given year n, NO$_x$ emissions from stationary combustion and off-road mobile source are calculated as follows:

$$E_n = \sum_{i,j,k} A_{i,j,k,n} \sum_m \left(X_{i,j,k,m,n} EF_{j,k,m} \right) \qquad (1)$$

where, i represents the province (municipality, autonomous region); j represents the economic sector; k represents the fuel type; m represents the technology type; n represents the year; E is the national NO$_x$ emission estimate in the year; A is the activity level (such as fuel consumption); X is the percentage of fuel consumption of technology m in total fuel consumption in sector j; and EF is the NO$_x$ emission factor.

[14] Emissions of NO$_x$ from on-road vehicles are calculated as follows:

$$E_n = \sum_{i,j,k} \left(VP_{i,j,n} \times X_{i,j,k,n} \times VMT_{i,j,n} \times FE_{i,j,n} \times EF_{j,k} \right) \quad (2)$$

where, i represents the province (municipality, autonomous region); j represents the vehicle type; k represents the control technology; n represents the year; VP is the vehicle population; X is the share of vehicles with control technology k in the vehicle type j; VMT is the annual average vehicle mileage traveled, in km/year; FE is the average fuel economy, in kg/km; and EF is the NO$_x$ emission factor, in g/kg.

3.1. Combination of Activity Rates and Emission Factors

[15] Using a similar approach to *Streets et al.* [2006], the activity data are developed from a wide variety of sources. Fuel consumption by sector and by province is derived from the China Energy Statistical Yearbook (CESY) [*National Bureau of Statistics of China* (*NBS*), 1998, 2001, 2004, 2005, 2006]. Technology distributions within each sector are obtained from Chinese statistics, technology reports, and an energy demand approach for the residential sector [*NBS*, 1996–2005; *China Mechanical Industry Association*, 1996–2006; *Zhou et al.*, 2003; China Cement Association, unpublished data, 2005; China Electricity Council, China's power generation statistics, unpublished data, 2005]. As shown in equation (2), vehicular NO$_x$ emissions are closely related to vehicle technology distribution, fuel type, fuel economy, and annual mileage traveled, which are estimated by a transportation model [*He et al.*, 2005]. The detailed approaches for combination of activity data at the technology level have been described in *Streets et al.* [2006]. However, on the basis of the differences in the processes that form NO$_x$ and CO, we have made the following three additional improvements to the categorization of sources that enable a more accurate representation of NO$_x$ emissions to be made:

[16] 1. Adjust the classification of coal devices (for the original classification scheme, see *Streets et al.* [2006]). We now divide pulverized coal-fired boilers in the power sector into four subcategories based on boiler capacity and combustion technology that have different levels of NO$_x$ emissions.

[17] 2. Segregate liquid and gaseous fuels more carefully. These high-quality fuels are combusted efficiently in most stationary combustion equipment types, generating very little CO but considerable NO$_x$. So in the new model we have classified liquid and gaseous fuels by fuel type and by sector and applied corresponding emission factors, instead of using just one uniform source category for each of these fuels, as in our CO model.

[18] 3. Remove industrial processes that release by-product gas containing much CO but little NO$_x$, such as coke production, iron and steel production, and synthetic ammonia production.

[19] Several previous inventory studies developed NO$_x$ emission factors by fuel and by sector for China [*Kato and Akimoto*, 1992; *Hao et al.*, 2002; *Streets et al.*, 2003]. Generally, those NO$_x$ emission factors relied on international databases, because of the lack of local measurements. In this work, we perform a critical reexamination of emission factors, based on newly available measurements in China or estimations based on the actual technology level and practice. Thus the new emission factors are much more representative of actual emission rates in China than those that have been used in previous work. Sections 3.2–3.6 document the methodologies and assumptions used in our BGE scenario and discuss possible variations on these assumptions.

3.2. Inconsistency in China's Energy Statistics

[20] Building a regional emission trend for China must rely heavily on periodic government statistical publications like CESY for the year-to-year activity changes. However, when CESY data are examined for a 10-a period and incorporated into our model, problems arise. For example, it is found that the sum of provincial fuel consumption values from the provincial energy balance table is different from the fuel consumption presented in the national energy balance table, especially for coal and diesel oil, which are believed to be the main contributors to China's NO$_x$ emissions. Table 2 presents the differences in coal and diesel consumption between the two tables during the 10-a period. For the first 3 a, coal consumption in the two tables matches quite well across all sectors. After that, the two tables still match well in the power sector, but begin to show significant differences for other sectors. The numbers in the provincial table rise more rapidly. The difference reaches a peak in the year 2002. Total coal consumption in the provincial table is 20% higher than in the national table in 2002.

[21] The inconsistencies between the two tables are intriguing. In the national table, China's total coal consumption (for combustion use only, not including consumption as raw material) apparently decreased by 13% from 1996 to 2000. In the provincial table, on the other hand, coal consumption declined by only 2% during the same period. Obviously, NO$_x$ emissions calculated using these different energy balance tables will generate very different trends. That exceptional decline in the national table has been doubted by *Sinton* [2001] and partly attributed to the fact that the National Bureau of Statistics failed to report the coal output from nominally closed small coal mines. It is also possible that the difference comes from conflicting statistical

Table 2. Differences Between the Provincial Energy Balance Table and the National Energy Balance Table in Various Issues of the China Energy Statistical Yearbook, 1995–2004[a]

	1995	1996	1997	1998	1999	2000	2001	2002	2003	2004
Coal total[b]	1.02	1.00	1.05	1.08	1.10	1.13	1.19	1.20	1.18	1.18
Power	1.00	1.00	1.00	0.98	0.97	0.96	1.01	0.99	1.00	1.01
Heating	1.00	1.00	1.02	1.00	1.04	1.13	1.26	1.29	1.11	1.09
Industry[c]	1.00	0.97	1.05	1.10	1.18	1.32	1.32	1.44	1.39	1.23
Residential[d]	1.04	1.01	1.11	1.35	1.31	1.29	1.35	1.35	1.30	1.32
Diesel total[e]	0.85	0.83	0.83	0.79	0.77	0.78	0.81	0.77	0.85	0.81

[a]Values represent the ratios between the numbers in the provincial table and the national table.

[b]Sum of thermal power, heating supply, and total final consumption in the balance table, which are most closely associated with NO$_x$ emissions.

[c]Industry consumption, after subtracting nonenergy use.

[d]Total final consumption, except industry.

[e]Total final consumption in the balance table.

approaches used in the two tables. However, at the present time there is no further way to confirm or refute these possibilities. In the present study, data in the provincial energy balance table are used to represent coal consumption at provincial level in each year in the BGE scenario; coal consumption data in the national table are used as the assumption of alternative energy scenario 1 (E1), as part of the sensitivity analysis.

[22] Significant differences in diesel consumption data in the two tables are also found over the years. Unlike coal consumption, diesel consumption in the provincial table is lower than that in the national table. The average ratio is around 0.80, differing by about 0.05 across the period. For example, in the national table, total diesel consumption increases to 99.0 million tons in the year 2004, while the sum of values in the provincial table is only 78.8 million tons. Because the NO$_x$ emission rate from diesel is larger than for other fuels (see detailed description later), the 20 million tons difference will affect the national NO$_x$ emission estimates significantly. We examined the data carefully and found that the changes in diesel production, import amount, export amount, and storage presented in the two tables match well across the period. We further investigated data in the China Petrochemical Corporation Yearbook and the China Chemical Industry Yearbook [*China Petroleum and Chemical Industry Association*, 2005; *China Petrochemical Corporation*, 2005]. Diesel production reported by the petroleum industry also matches well with the data in the national energy table, which suggests that the diesel production data are reliable. However, we found a large discrepancy in the interprovince transportation data in the provincial energy table. For example, for 2004, the sum of diesel "import(s) from other province(s)" is 68.3 million tons, while the sum of diesel "export(s) to other province(s)" is 86.4 million tons; this suggests that the 18 million tons "lost" from interprovince transportation is the cause of the inconsistency between the two tables. It is not completely clear where the problem originates, but we believe that the diesel consumption in the national table is more reliable.

[23] The actual diesel consumption in the late 1990s in China might even be higher than reported in the national energy table. In 1998, the Chinese government banned imported fuel to protect the domestic petroleum industry from fuel dumping. *Fisher-Vanden et al.* [2004] indicated that this policy led to illegal smuggling of diesel fuel that does not show up in the statistics. However, it is impossible to know how much diesel might have been illegally imported. In this work, we use the diesel consumption in the national table and the shares from the provincial table to represent the consumption at provincial level in each year in the BGE scenario. Further, we use the diesel consumption in the provincial table as an assumption of alternative energy scenario 2 (E2), to explore the impact of activity data inconsistency on NO$_x$ trends.

3.3. Decomposition of Gasoline and Diesel Fuel Consumption Data

[24] Another difficulty arises when trying to decompose the gasoline and diesel consumption data. It is estimated that 97% of gasoline and 45% of diesel were burned in various types of vehicles in China in 2000 [*Yang*, 2001]. So

the corresponding gasoline and diesel consumption amounts should be attributed to the transportation sector. However, because of the statistical approach followed in CESY, gasoline and diesel consumption in the transportation sector only reflects fuel used in commercial transportation activities. Fuel used in factories or personally owned vehicles is listed within the separate categories of industry, residential, etc. [*Zhou et al.*, 2003]. Because of the need to consider the variety of in-use vehicles in China and their widely differing emission rates, we classified on-road vehicles into light-duty gasoline vehicles (LDGV), light-duty gasoline trucks up to 6,000 lb gross vehicle weight (LDGT1), light-duty gasoline trucks with gross vehicle weight 6,001–8,500 lb (LDGT2), light-duty diesel trucks (LDDT), heavy-duty gasoline vehicles (HDGV), heavy-duty diesel vehicles (HDDV), and motorcycles, corresponding to the classification method in the U.S. EPA's MOBILE emission factor model. To be thorough in our estimation of emissions, we also include rural vehicles in our calculation. It is not possible to derive the fuel consumption for each vehicle type from CESY. As an alternative approach, we estimate fuel consumption from vehicle population (VP), annual average vehicle mileage traveled (VMT), and fuel economy (FE) for each type of vehicle. The VP of each vehicle type is calculated from total VP and the shares of each vehicle type. For vehicle shares, we assume that the share in a given year is the average value of sales shares of the past 15 a [*China Association of Automobile Manufacturers*, 1991–2005]. VMT of each vehicle type is derived from freight traffic volume (tonnage or ton-km) and passenger traffic volume (passengers or passenger-km). FE is based on a combination of labeled fuel economy data and other investigations. The full details of the model used and the methodological approach are described elsewhere [*He et al.*, 2005].

[25] The model-derived vehicular gasoline consumption is within 5% of the national total gasoline consumption, and the model-derived vehicular diesel consumption accounts for 35–55% of national total diesel consumption during the period 1995–2004. In addition to vehicular use, diesel fuel is widely used in tractors, off-road equipment, locomotives, vessels, and boilers in China, accounting for the other 45–65% of total diesel consumption. We encounter difficulties, however, when trying to obtain diesel consumption data by equipment type. There is no such information available at provincial level. *Yang* [2001] present the share of national diesel consumption by equipment, so we first subtract the vehicular diesel consumption derived by our model from total diesel consumption and then allocate the remaining diesel consumption to each equipment type using the shares reported by *Yang* [2001].

3.4. Coal Combustion
3.4.1. Power Plants

[26] Power plants are the largest coal consumer in China and are believed to be the largest contributor to China's NO$_x$ emissions [*Hao et al.*, 2002; *Streets et al.*, 2003]. China's power generation grew very rapidly during the period 1995–2004. Thermal power generation increased from 802 billion kWh in 1995 to 1,796 billion kWh in 2004 [*NBS*, 1998, 2001, 2004, 2005, 2006]. Over the same period, energy use for thermal power generation increased from 338 million tons of coal equivalent (tce) in 1995 to
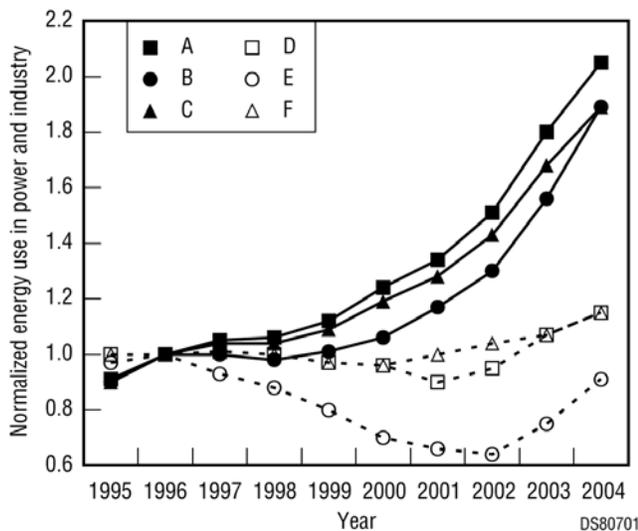
Figure 1. Trends of energy use in power plants and industry in China. All data are normalized to the year 1996. Line A presents the trend of thermal power generation in China, line B presents the energy consumption in China's power plants from China's energy statistics, line C presents the calculated energy consumption in China's power plants constrained by gradually improved energy efficiency, line D presents the industrial coal consumption from the sum of provincial energy balance table, line E presents the industrial coal consumption from the national energy balance table, and line F presents the extrapolated industrial coal consumption for 2001–2002 using a basic linear function.

706 million tce in 2004 [*NBS*, 1998, 2001, 2004, 2005, 2006]. Figure 1 shows the trends of thermal power generation and its energy use in China. All data are normalized to the year 1996, which is the year in which the GOME instrument was launched, in order to compare with the satellite data. Trends of thermal power generation and its energy use diverge after 1996. Thermal power generation shows the higher growth trend; average energy efficiency in power plants improved 14% during 1996 and 2000, leading to a lower growth trend for fuel consumption. After 2000, energy efficiency remained stable for several years, but improved again, by 7%, from 2002 to 2004.

[27] Why did the average energy efficiency in power plants change so dramatically? There are many factors that can impact the average energy efficiency in power plants, such as advances in combustion technology, improvements in plant management, changes in fuel quality, and so on, but, to our knowledge, none of them can explain these dramatic changes. One possible explanation concerns China's policy to phase out small thermal power generation units (STPGUs) with capacity less than 50 MW after 1995. Up to 2001, 12.3 GW of STPGUs were closed, accounting for 5% of the total thermal power capacity in 2001 [*Xue et al.*, 2003]. Because the energy efficiencies of STPGUs are usually 1.5–2 times lower than large units, this progress could significantly improve the average energy efficiency of China's power sector in a short time. However, new STPGUs were returned to the market after 2002, because of rapidly increasing power demands, resulting in a decrease

of average energy efficiency. Although we cannot be sure if the dramatic change of energy efficiency in power plants really happened, we can say that if the energy efficiency improved gradually, say by the recent value of 7% throughout 1995–2004 at a constant growth rate, then the trend of energy use will be different (compare lines B and C in Figure 1) and a different emission trend will result. Hence we use line C of Figure 1 as the assumption of alternative energy scenario 3 (E3), to explore the impact of energy efficiency in power plants on NO$_x$ trends.

[28] NO$_x$ emission rates in coal-fired power plants vary by boiler size, level of NO$_x$ control technology, and coal quality, all of which have changed significantly in China in the past 10 a. The market share of large boilers, for instance, has increased rapidly. Boilers with capacity larger than 300 MW accounted for 24% of total capacity in 1995 and 44% in 2004. In contrast, boilers with capacity less than 100 MW accounted for 38% in 1995, but only 27% in 2004 (China Electricity Council, China's power generation statistics, unpublished data, 2005). LNB technology is the only NO$_x$ control technology widely used in China's power plants, and its penetration increased gradually over time under the strengthened requirements of China's NO$_x$ emission standards [*State Environmental Protection Administration of China* (*SEPA*), 1996, 2003].

[29] Most previous studies used a single value to represent the average NO$_x$ emission rate of coal-fired power plants, commonly 10 g/kg [*Kato and Akimoto*, 1992; *Hao et al.*, 2002; *Streets et al.*, 2003]. *Tian* [2003] studied more than 100 coal-fired power plant boilers and determined that the average NO$_x$ emission factor was 8.85 g/kg, representing a mix of boilers with and without LNB. However, when generating the NO$_x$ emission trends for 1995–2004, we clearly must include the effect of the trend in technology innovation on emission factors. In this work, we classify boilers into four categories, based on boiler size and LNB technologies, which are listed in Table 3. NO$_x$ emission factors for each boiler type are derived from the review of *Tian* [2003]. Furthermore, we made the following assumptions for LNB penetration in the BGE scenario, based on a review of current practice in China [*Bi*, 1998; *Hao et al.*, 2002; *Li*, 2005; *Zhang et al.*, 2005]: (1) All existing and new boilers with capacity equal to or larger than 300 MW are equipped with LNB by 1995; (2) boilers smaller than 300 MW but equal to or larger than 100 MW were not equipped with LNB before 1997, but LNB began to be installed after 1997 under SEPA requirements [*SEPA*, 1996], increasing gradually from 0% in 1997 to 80% in 2004; and (3) no boilers smaller than 100 MW are equipped with LNB during the period.

[30] Regarding the emission factors for each boiler type presented in Table 3, the average emission factors for China's coal-fired power plants during 1995–2004 were calculated, using the above assumptions and the boiler size distribution data (China Electricity Council, China's power generation statistics, unpublished data, 2005). The average NO$_x$ emission factors of coal-fired power plants in China declined gradually from 8.9 g/kg in 1995 to 7.4 g/kg in 2004, decreasing by 17% in 10 a (see Figure 2). The decrease can mainly be attributed to the increased share of large boilers and the spread of LNB technology. However, it should be noted that the assumptions about LNB penetra-

Table 3. Summary of NO$_x$ Emission Factors for Different Types of Coal-Fired Power Plants

Boiler Size	Combustion Technology	Bituminous Coal, mg/Nm^3	Anthracite Coal or Lean Coal, mg/Nm^3	Average Emission Factor[a]	
				mg/Nm^3	g/kg[b]
<100 MW	without LNB	1300	1800	1400	10.5
≥100 MW, but <300 MW	without LNB	1100	1500	1180	8.85
≥100 MW, but <300 MW	with LNB	650	1300	780	5.85
≥300 MW	with LNB	650	1100	740	5.55

[a]Based on the assumption that 80% of coal is bituminous and the rest is anthracite and lean coal.
[b]Assuming 6% O_2 in the flue gas, and the heat value of coal is 5000 Kcal/kg to convert the unit from mg/Nm^3 to g/kg. 1 mg/Nm^3 = 0.75 g/kg.

tion are based on the description of China's status in the literature [*Bi*, 1998; *Hao et al.*, 2002; *Li*, 2005; *Zhang et al.*, 2005], not on statistical sampling data. To examine the sensitivity of the LNB assumption, we include an alternative emission factor scenario 1 (F1), which assumes that the NO$_x$ emission factor for coal-fired power plants remained constant at 8.9 g/kg.

3.4.2. Industrial Coal Combustion

[31] The industry sector is another important coal consumer, responsible for about one third of national coal consumption. The trend of coal consumption in the industry sector during the period 1995–2004, in particular the apparent decline from 1996 to 1999, has been the source of much confusion. The reasons for it are still debated, but are variously attributed to the following factors: structural change, energy efficiency improvements, and inaccurate statistics [*Sinton and Fridley*, 2000; *Sinton*, 2001; *Zhang*, 2003; *Fisher-Vanden et al.*, 2004]. The decline continued and accelerated up to 2001, drawing a concave curve between 2000 and 2002 (see lines D and E in Figure 1). In contrast, almost all energy-consuming industrial production increased markedly from 2000 to 2002 (pig iron increased by 30%, cement 21%, paper 88%, chemical fertilizer 19%, synthetic ammonia 9%, and chemical fibers 43% [*NBS*, 1996–2005]). The abnormal trends during 2000 and 2002 need to be further investigated. We construct an alternative energy scenario 4 (E4) by extrapolating industrial coal consumption for 2001–2002 using a basic linear function (line F in Figure 1).

[32] There is a wide variety of types of coal-burning equipment in China's industry sector, all with different emission factors. We include six types of coal combustion devices in our treatment of the industrial sector, including three types of boilers (fluidized bed furnaces (FBF), automatic stokers, and hand-feed stokers) and three types of kilns (cement kilns, lime kilns, and brick kilns). Detailed information on these devices has been described in our previous work [*Streets et al.*, 2006]. The market shares of each type of technology by province are derived from a wide literature review [*China Mechanical Industry Association*, 1996–2006; *NBS*, 1996–2005; *Yan*, 1997; *Zhou et al.*, 2003; China Cement Association, unpublished data, 2005].

[33] The technology distribution of industrial boilers has been relatively stable during recent years. Stokers are the dominant industrial boiler type, comprising more than 90% of the market share. Peking University (PKU) [*Peking University*, 2001] reported that different types of automatic stokers produce 2.8–4.2 g NO$_x$ per kg coal burned and hand-feed stokers produce 3.8 g/kg, which is very comparable with the values of 2.8–5.5 g/kg for automatic stokers

and 4.5 g/kg for hand-feed stokers reported in the AP-42 database [*U.S. Environmental Protection Agency*, 1996]. In this work, we use 4.0 g/kg and 3.8 g/kg, for automatic and hand-feed stokers, respectively.

[34] Unlike industrial boilers, the technology in cement kilns has changed dramatically in the past 10 a. Cement production in shaft kilns accounted for 81% of the total production in 1995. However, in the late 1990s a new type of rotary kiln, called the "new-dry" process in China, began to replace older shaft kilns and rotary kilns. By 2004 the share of new-dry process kilns had grown to 32%, while the share of shaft kilns had dropped to 59%. The remaining 8% are other types of rotary kilns (China Cement Association, unpublished data, 2005).

[35] NO$_x$ emission rates in different types of kilns can vary dramatically. Emission factors are relatively low in shaft kilns, because the high concentration of CO in the combustion gas produces a reducing atmosphere that restrains the formation of NO$_x$ [*Streets et al.*, 2006]; NO$_x$ emissions from rotary kilns are much higher. *Su et al.* [1998] reported NO$_x$ emission factors for cement kilns of about 0.3 g/kg-cement for shaft kilns and 3.4 g/kg-cement for rotary kilns (equal to 1.7 and 18.5 g/kg-coal, respectively). The *Chinese Research Academy of Environmental Sciences* [2003] measured 16 new-dry process kilns and obtained an average value of 2.8 g/kg-cement (15.3 g/kg-coal). Using the above emis-
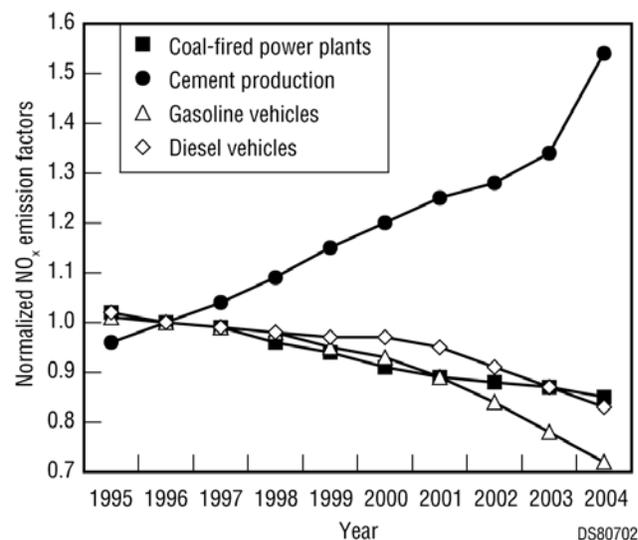

Figure 2. Trends of NO$_x$ emission factors for several important source types. All data are normalized to the year 1996.

Table 4. NO$_x$ Emission Factors for Coal Combustion Devices in the Industrial and Residential Sectors

Sector or Usage	Technology	NO$_x$, g/kg
Industry/boiler	fluidized-bed furnace	7.5
Industry/boiler	automatic stoker	4.0
Industry/boiler	hand-feed stoker	3.8
Industry/cement production	shaft kiln	1.7
Industry/cement production	new-dry process	15.3
Industry/cement production	other rotary kiln	18.5
Industry	lime kiln	1.7
Industry	brick kiln	4.7
Residential	automatic stoker	4.0
Residential	hand-feed stoker	3.8
Residential	coal stove	0.91

sion factors and data on the market shares of different types of kilns from China Cement Association (unpublished data, 2005), the average NO$_x$ emission factor for China's cement industry can be calculated. We estimate that the average NO$_x$ emission factor for the cement industry grew from 4.6 g/kg-coal in 1995 to 7.4 g/kg-coal in 2004, increasing by 61% in 10 a (see Figure 2), leading to rapid growth in NO$_x$ emissions from cement plants.

[36] There is very limited information on emission factors for lime kilns and brick kilns. In this work, we assume that lime kilns have the same NO$_x$ emission factors as shaft cement kilns, due to the similar technical process, with high uncertainty. The emission factor for brick kilns, 4.7 g/kg-coal, is based on limited measurements by *Tang et al.* [1995], also with high uncertainty. We assume that the emission factors for lime kilns and brick kilns do not change over time. To evaluate the sensitivity of NO$_x$ emission factors for industrial coal combustion, we include an alternative emission factor scenario 2 (F2) that uses the value of 8 g/kg for all industrial coal combustion equipment, as assumed in the TRACE-P inventory [*Streets et al.*, 2006].

3.4.3. Residential Sector

[37] The share of residential coal use in total coal consumption declined from 18% in 1995 to 10% in 2004. Energy statistics for the residential sector are unreliable [*Sinton et al.*, 2004]. However, because the residential sector has not been shown to be a large contributor to China's NO$_x$ emissions in previous studies [*Hao et al.*, 2002; *Streets et al.*, 2003], we simply used the China statistical data in our calculations and did not generate any alternative scenarios. The shares of stokers and stoves in the residential sector are estimated using an energy demand approach, which has been described by *Streets et al.* [2006]. For coal combustion in residential stokers, we use the same NO$_x$ emission factors as for industrial stokers. For the combustion of coal in stoves and cookers of various types, there is no updated information available, and therefore the measurements of *Zhang et al.* [2000] are used. Emission factors are assumed to be constant over time. Table 4 summarizes the NO$_x$ emission factors for individual industrial and residential coal combustion technologies used in this work.

3.5. Other Stationary Combustion Sources

[38] Besides coal, three types of solid fuels (wood, crop residues, and coke) and nine types of liquid and gaseous fuels (crude oil, kerosene, diesel, fuel oil, LPG, other petroleum products, refinery gas, natural gas, and coke oven gas) are burned in China and are taken into account

in this work. Activity rates by fuel type and sector were obtained from the CESY [*NBS*, 1998, 2001, 2004, 2005, 2006], except for gasoline and diesel. All gasoline fuels are attributed to mobile source usage, and diesel consumption for stationary combustion is derived from the methodology described in section 3.2. The measurements of *Zhang et al.* [2000] are used for emission factors of wood and crop residues, while other emission factors by fuel type and by sector are taken from *Hao et al.* [2002] and assumed to be constant over time.

3.6. Mobile Sources
3.6.1. On-Road Vehicles

[39] Classification and activity rates of on-road vehicles are derived from the methodologies described in section 3.2. Emission factors for each category of vehicle for each province are derived using the MOBILE5b model, as described for China in the work of *Fu et al.* [2001], which are considered to be representative of average emission rates in the late 1990s in China. We used those values as the base emission rates for the pre-1999 vehicles in the fleet. China adopted vehicle emission control measures in 1999 [*He et al.*, 2002]. In large cities like Beijing and Shanghai, where a good proportion of new vehicles are purchased, a set of new emission standards was implemented in 1999, which correspond to Euro-I standards; these standards spread to the whole of China in 2001. New vehicles joining the fleet since 1999 have new emission control technologies and lower NO$_x$ emission factors. Beijing and Shanghai implemented Euro-II standards in 2003, which spread to the whole of China in 2004, thereby reducing NO$_x$ emission factors further. These standards are included in the MOBILE5b model to adjust the base emission rates for new vehicles coming into the fleet after 1999. On the basis of the assumptions above, the year-by-year emission factors for each vehicle type are estimated by the MOBILE5b model at provincial level. Emission factors are originally presented in units of g/km, then converted to g/kg of fuel according to the fleet average fuel economy data of *He et al.* [2005].

[40] The overall situation is that the fleet average NO$_x$ emission factors decreased gradually as the share of new vehicles increased. Average NO$_x$ emission factors for gasoline vehicles declined from 31.8 g/kg in 1995 to 22.8 g/kg in 2004, decreasing by 28% during the 10-a period. Average NO$_x$ emission factors for diesel vehicles declined by 18% during the same period, from 72.3 g/kg in 1995 to 59.1 g/kg in 2004 (Figure 2). The year-by-year NO$_x$ emission factors estimated in this work for each type of vehicle are listed in Table 5. We also include an alternative emission factor scenario 3 (F3) to examine the sensitivity of the NO$_x$ emission trends to vehicle emission rate, assuming that vehicle emission factors remained at the level of the late 1990s throughout the period. Under this scenario, average NO$_x$ emission factors for gasoline vehicles decrease from 31.8 g/kg in 1995 to 27.3 g/kg in 2004, and average NO$_x$ emission factors for diesel vehicles decrease from 72.3 g/kg in 1995 to 70.5 g/kg in 2004.

3.6.2. Off-Road Mobile Sources

[41] For nonvehicular diesel fuel use, an emission factor of 9 g/kg was applied for all diesel consumption in the TRACE-P inventory, which represents the typical NO$_x$ emission level in diesel-fueled boilers. However, diesel

Table 5. NO$_x$ Emission Factors for Mobile Sources[a]

Combustion Equipment	Fuel	1998	2001	2004
LDGV	gasoline	28.1	25.6	21.2
LDGT1	gasoline	34.7	30.9	25.5
LDGT2	gasoline	43.6	42.8	39.3
HDGV	gasoline	33.4	33.2	31.8
Motorcycles	gasoline	7.1	7.1	5.0
Gasoline vehicle average	gasoline	30.9	28.0	22.8
LDDT	diesel	19.8	17.0	14.4
HDDT	diesel	79.1	78.1	67.2
Diesel vehicle average	diesel	69.8	65.0	59.1
Rural vehicles and tractors	diesel	45	45	45
Off-road equipment	diesel	48	48	48
Locomotives	diesel	75	75	75
Vessels	diesel	55	55	55

[a]Unit is g/kg.

boilers only comprise 15–20% of total diesel fuel consumption. The NO$_x$ emission rates for internal diesel engines, such as tractors, off-road equipment, locomotives, and vessels, are much higher than for boilers. In this work, NO$_x$ emission factors for those types of equipment are taken from U.S. studies [*Kean et al.*, 2000], because of the lack of local measurements.

3.7. Monthly Variations in Emissions

[42] To develop the monthly variability of NO$_x$ emissions over China, we have examined the potential monthly variations of energy use for each sector. In the TRACE-P inventory, *Streets et al.* [2003] developed seasonal variations of residential energy consumption, assuming a dependence of stove operation on provincial monthly mean temperatures. We use the same methodology to generate monthly profiles of NO$_x$ emissions for the residential sector. No seasonal variation was considered for power generation and industrial energy use in the TRACE-P inventory because of a lack of such information; however, we have now obtained monthly data on power generation, cement production, and industrial GDP for the period 1995–2004 [*Beijing Huatong Market Information Co. Ltd.*, 1996–2004; *China Statistical Information and Consultancy Center*, 1996–2004]. We use these data to generate monthly, provincial-level profiles of NO$_x$ emissions for the power sector, the cement industry, and other industries, for the whole period. National average data were used where provincial data were lacking during the period 1995–1999. We assume that transportation energy use and emissions remain constant from month to month, in the absence of any information to the contrary.

4. Results

4.1. Interannual and Seasonal Emission Trend of the BGE Scenario

[43] On the basis of the methodology described above, we calculate anthropogenic NO$_x$ emissions from fuel combustion in China for the period 1995–2004. We estimate that NO$_x$ emissions in China were 10.9 Tg in 1995 and 18.6 Tg in 2004, increasing by 70% during the period, at a 6.1% annual average growth rate. The growth rate itself was accelerating during the period. NO$_x$ emissions increased by 7% during the first 3 a and 40% during the last 3 a. The largest increment occurred in 2004, the final year of our

time period, at 15%. In contrast, NO$_x$ emissions were almost stable during 1996 and 1998, only increasing by ∼1% annually.

[44] We have also examined the seasonal variations of NO$_x$ emissions in this study. Figure 3 presents the monthly profile of China's NO$_x$ emissions by sector. Significant monthly variations were found in each of the sectors. For example, the ratio of industrial emissions in the month with highest emissions (December) to industrial emissions in the month with lowest emissions (February) is 1.65. For total anthropogenic emissions, maximum values generally occur in January and December because of domestic heating needs, and minimum values generally occur in April and May. Emissions in July are slightly higher than in April and May because of the higher load of power generation in summer. The ratio of emissions in December to emissions in July is 1.3, higher than the value of 1.2 given by *Streets et al.* [2003].

[45] An uncertainty analysis was performed on the NO$_x$ emission inventory. The two crucial factors that influence the accuracy of the emission estimates are activity level and emission factor. This study applied the same method as used in the TRACE-P inventory [*Streets et al.*, 2003] to calculate the uncertainty levels and their time variation. The method was described in detail by *Streets et al.* [2003, section 3.5]. Results showed that the uncertainty of NO$_x$ emissions in this present work is ±29–32% in the period of 1995–2004, measured as 95% confidence intervals. This level of uncertainty is comparable with the ±24% uncertainty reported in the TRACE-P inventory. The uncertainty of emissions from residential biofuel combustion is the highest, at about ±164%. The uncertainty of emissions from the power sector is the lowest, at ±37%. The uncertainty increases slightly over time because of the increasing share of transportation emissions, which have higher uncertainties.

4.2. Driving Forces of Emission Growth

[46] It is confirmed that China's NO$_x$ emissions increased rapidly during the 10-a period 1995–2004. Because we
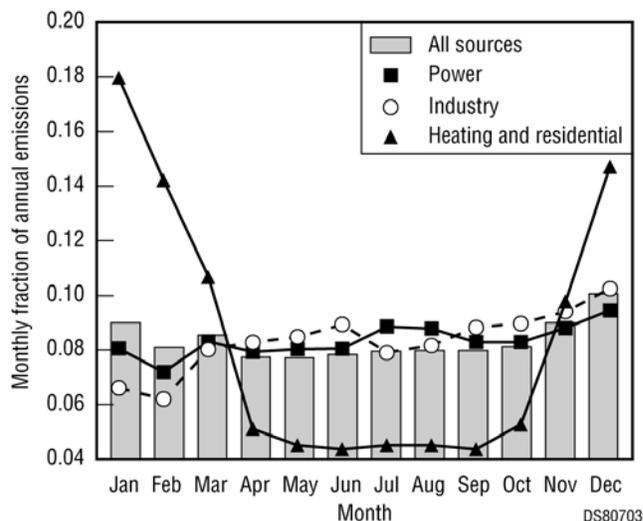

Figure 3. Monthly profile of NO$_x$ emissions by sector. *Y* axis values represent the share of the monthly emissions in the year.

Table 6. NO$_x$ Emissions by Sector and Source Type in China, 1995–2004[a]

	1995	1996	1997	1998	1999	2000	2001	2002	2003	2004	Annual Rate, %
Power											
Coal	3.9	4.3	4.2	4.1	4.1	4.2	4.5	5.0	5.9	6.9	6.5
Other fuels	0.11	0.12	0.11	0.12	0.12	0.12	0.11	0.12	0.12	0.18	5.9
Subtotal	4.1	4.4	4.3	4.2	4.2	4.3	4.6	5.1	6.0	7.1	6.6
Heating	0.46	0.51	0.50	0.50	0.53	0.53	0.68	0.75	0.82	0.97	8.7
Industry											
Coal	1.9	1.9	1.9	2.0	1.9	2.0	1.9	2.0	2.3	2.7	4.3
Other fuels	1.1	1.2	1.2	1.3	1.4	1.5	1.5	1.6	1.8	2.0	6.6
Subtotal	3.0	3.1	3.1	3.2	3.3	3.4	3.4	3.6	4.1	4.7	5.2
Residential											
Coal	0.49	0.51	0.50	0.48	0.42	0.39	0.40	0.43	0.39	0.41	−1.7
Biofuels	0.51	0.44	0.44	0.47	0.47	0.47	0.51	0.57	0.57	0.59	1.7
Other fuels	0.04	0.05	0.05	0.05	0.06	0.07	0.08	0.09	0.09	0.11	11.4
Subtotal	1.0	1.0	1.0	1.0	0.95	0.93	0.99	1.1	1.1	1.1	0.7
Transportation											
Gasoline vehicles	0.89	0.90	0.88	0.91	0.92	0.99	1.0	1.0	1.1	1.1	2.6
Diesel vehicles	0.72	0.78	0.87	0.99	1.1	1.2	1.4	1.7	1.9	2.1	13.0
Off-road mobile sources	0.73	0.79	0.78	0.87	1.0	1.1	1.1	1.2	1.2	1.4	7.8
Subtotal	2.3	2.5	2.5	2.8	3.1	3.4	3.5	3.8	4.2	4.7	8.0
China total	10.9	11.5	11.5	11.7	12.1	12.6	13.2	14.4	16.2	18.6	6.1

[a]Unit is Tg NO$_2$.

have used a bottom-up methodology to estimate emissions, we have tools to explore the nature of the driving forces of NO$_x$ emission growth in detail. Table 6 summarizes the NO$_x$ emission estimates by sector and fuel type from 1995 to 2004. Except for the residential sector, all sectors present a synchronous growth of NO$_x$ emissions; however, the key factors that influence the trend change over the period.

[47] China's coal consumption decreased after the year 1996, which resulted in the decrease of total energy consumption. However, NO$_x$ emissions increased from 11.5 Tg in 1996 to 12.6 Tg in 2000, at an annual average rate of 3% and without showing a decrease for any individual year. *Akimoto et al.* [2006] attributed this to the increasing trend of power plant emissions during the period. We believe that this cannot be the correct explanation for the following two reasons: (1) The increasing NO$_x$ emission trend during 1996–2000 was mainly driven by the transportation sector, because the vehicle population increased from 9.8 million in 1995 to 15.6 million in 2000, causing NO$_x$ emissions from the transportation sector to increase from 2.5 Tg to 3.4 Tg and thereby contributing 82% of the total increase during that period, and (2) although industrial coal consumption decreased during 1996–2000, cement production increased by 18%, and as discussed in section 2, cement kilns generate much more NO$_x$ than industrial boilers per ton of coal burned. The increase in NO$_x$ emissions from cement kilns caused NO$_x$ emissions from industrial coal consumption to remain relatively stable during 1996–2000. In contrast, although coal consumption in the power sector increased from 489 Mt in 1996 to 524 Mt in 2000, NO$_x$ emissions from power plants were stable because of the increasing penetration of LNB technologies.

[48] China's NO$_x$ emissions started their dramatic growth after the year 2000, which was the year when China's economy began to boom and infrastructure investments grew rapidly. Explosive growth in power generation then became the driving force behind the NO$_x$ emission increase. Emissions from power plants increased from 4.3 Tg in 2000 to 7.1 Tg in 2004, up by 65% in 4 a, and this contributed 47% of the total increase during this period. Industrial

emissions increased from 3.4 Tg to 4.7 Tg and contributed 22% of the total increase. Vehicle numbers increased by 80%, but NO$_x$ emissions in the transportation sector only increased by 38% because of the implementation of vehicle emission standards.

4.3. Comparison of the Interannual Trends of the Inventory and Satellite Data

[49] *Richter et al.* [2005] derived the temporal evolution of tropospheric NO$_2$ columns from GOME and SCIA-MACHY satellite retrievals for the ECC region from 1996 to 2004 (the satellite retrievals change from GOME to SCIAMACHY starting in March 2003). The domain of their region extends from 30°N, 110°E to 40°N, 123°E. GOME and SCIAMACHY are satellite-borne spectrometers observing the upwelling radiance from the atmosphere, as well as the unattenuated solar irradiance in the UV and visible spectral regions. Both instruments are in near-polar, Sun-synchronous orbits, taking measurements at about 1000 and 0930 local time, respectively. The spatial resolution of the measurements is 320×40 km^2 for GOME and 60×30 km^2 for SCIAMACHY. Using the differential optical absorption spectroscopy (DOAS) method, non-light-path-corrected (slant) columns of NO$_2$ were determined from the measurements. They were then converted to tropospheric vertical columns through the application of air mass factors (AMFs) after removal of the stratospheric NO$_2$ columns. In this step, a priori assumptions on surface reflectivity, aerosol loading, and the vertical distribution of NO$_2$ were used, which have a significant impact on the results [see, e.g., *van Noije et al.*, 2006]. As the a priori was kept constant in the study of *Richter et al.* [2005], only changes in the parameters contribute to the uncertainties in the derived annual changes. For more details on this study, the reader is referred to *Richter et al.* [2005].

[50] While tropospheric NO$_2$ columns are important proxies for surface emissions over ECC, the relationship between column densities of NO$_2$ and emissions of NO$_x$ is by no means direct, depending on a variety of chemical and dynamical factors that have been estimated previously using
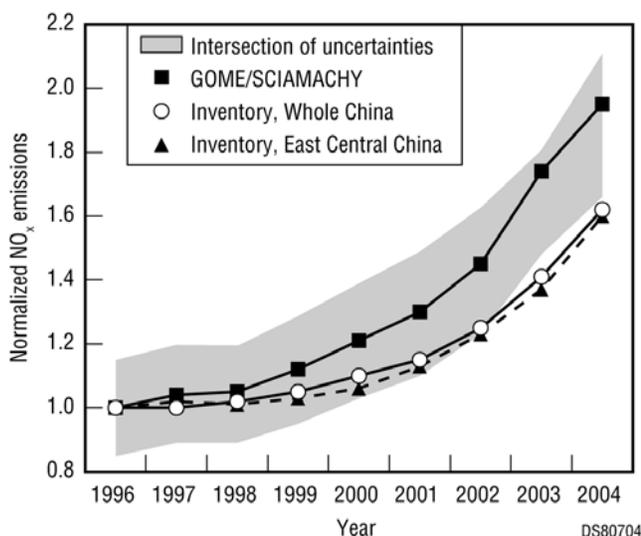
Figure 4. Temporal evolution of NO$_x$ emissions over China by inventory and satellite methods. All data are normalized to the year 1996.

three-dimensional chemical transport models [*Martin et al.*, 2003; *Jaeglé et al.*, 2005; *Wang et al.*, 2007]. The linkage of satellite measurements of NO$_2$ columns to NO$_x$ emissions are based on the assumptions of constant [NO$_2$]/[NO] ratio, constant [NO$_x$]/NO$_x$ emissions ratio, and constant NO$_x$ lifetime, where "constant" means in a given grid cell for a given month over the entire period. *Richter et al.* [2005] concluded, however, that the secular trends in NO$_2$ columns over ECC derived from space were mostly likely driven by changes in local emissions.

[51] The temporal evolution of the NO$_2$ columns derived by *Richter et al.* [2005] is compared with the inventory trends for China and the ECC region in Figure 4, relative to the 1996 values. Both the emission inventory data and the satellite observations indicate a continuous and accelerating growth rate between 1996 and 2004. However, the growth rate from the emission inventory is clearly lower than that from the satellite observations. From 1996 to 2004, NO$_x$ emissions over the ECC region increased by 61% according to the inventory, while a 95% increase in the NO$_2$ columns was obtained from the satellite observations during the same period. The largest inconsistency occurs in 2003, where the satellite columns increased by 20%, but the inventory only increased by 11%. Because 2003 is the year when the satellite data switched from GOME to SCIAMACHY, system error between the two instruments might be one possible explanation. Another major difference occurs between 1998 and 2000, where GOME retrievals increased by 15% in the ECC region, but the inventory only increased by 5%.

[52] The uncertainty of the satellite-derived tropospheric NO$_2$ columns is large (on the order of 40–50%), mainly as a result of the uncertainties in the assumptions that have to be made in the radiative transfer calculations when converting the slant columns from the DOAS analysis to vertical columns. For example, the retrieved seasonality of the NO$_2$ column can vary strongly depending on the assumptions made for aerosol loading and the vertical NO$_2$ profile, as

discussed by *van Noije et al.* [2006]. However, most of these error sources are systematic and cancel when relative changes are discussed, as is the case here. The uncertainty of the annual change rate is estimated to be on the order of 15% [*Richter et al.*, 2005]. The shaded area in Figure 4 represents the joint intersection of the ranges of uncertainty in the emission inventory and the satellite column data. The inventory and satellite data generally show good agreement within experimental and analysis error prior to 1998. After 1998, however, the two data sets begin to diverge; and by 2003 the accumulated difference between the two data sets causes departure of the inventory curve from the joint intersection area. This suggests that there must be some systematic errors that are not included in the joint uncertainty analysis.

4.4. Spatial Distribution

[53] Figure 5a shows the spatial distribution of NO$_x$ emissions in China in 2004 from the emission inventory, at a resolution of 30 min × 30 min. Emissions are distributed using various spatial proxies at 1 km × 1 km resolution [*Streets et al.*, 2003; *Woo et al.*, 2003]. The high emission regions are widespread across east China, from south of the Yangtze Delta region around Shanghai to north of Beijing. The Pearl River Delta (PRD) region of Hong Kong and Guangzhou and the Sichuan Basin also show high emission intensity. Figure 5b shows the averages of the tropospheric NO$_2$ columns derived from SCIAMACHY measurements for December 2003 to November 2004 [*Richter et al.*, 2005]. High NO$_2$ columns are shown across east China and the PRD region, corresponding to the high emission regions in Figure 5a.

4.5. Verification of Emission Inventories by Scenario Analysis and Satellite Data

[54] As described in section 3, we developed seven additional emission scenarios, in order to examine the sensitivity of the NO$_x$ emission estimates to key determining factors in the inventory: four scenarios for energy use (E1–E4) and three scenarios for emission factors (F1–F3). By means of this scenario analysis we can explore whether inconsistencies between the inventory and satellite observations can be explained by possible underestimation of emissions during various parts of the time trend. Table 7 tabulates the key assumptions of each scenario, and Table 8 compares NO$_x$ emissions in the ECC region for the BGE and the other seven scenarios. From the scenario analysis, we can draw the following conclusions that have implications for improving emission inventories:

[55] 1. Data sets on energy and fuel use should be used with care when compiling emission inventories for China. Both the E1 and E2 scenarios show lower NO$_x$ emissions than the BGE scenario and yield a larger discrepancy with the satellite trends, suggesting that the coal consumption data in the provincial energy balance table and the diesel consumption data in the national energy balance table may be the most accurate. This confirms conclusions from previous studies [*Streets et al.*, 2005, 2006; *Akimoto et al.*, 2006].

[56] 2. Minor anomalous trends in the energy statistics can affect NO$_x$ emission estimates. The impact could be important for an individual year but small for the whole
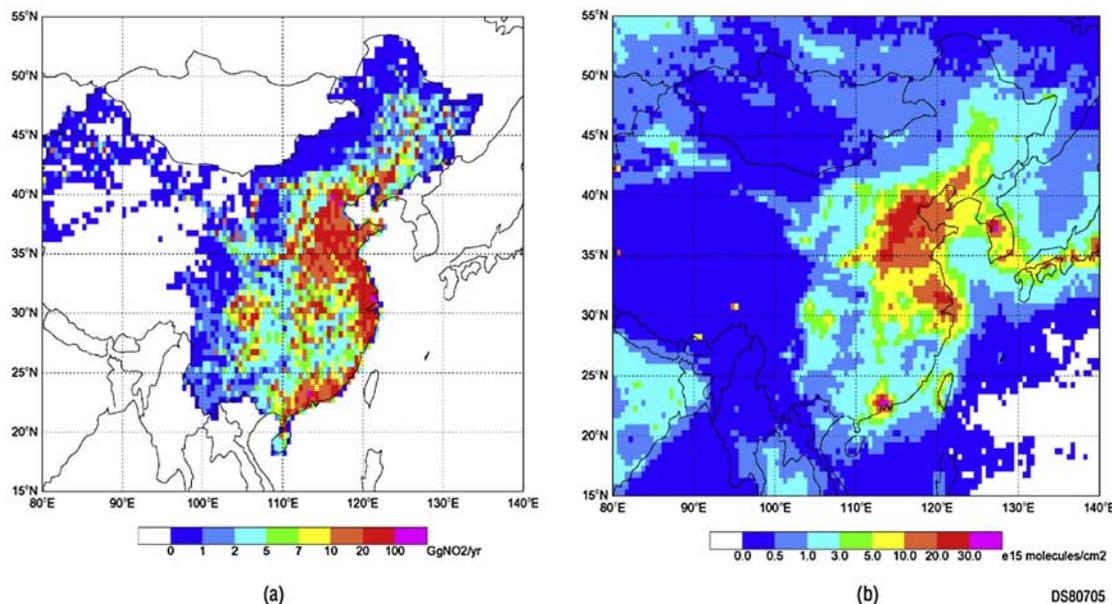
Figure 5. (a) Spatial distribution of the NO$_x$ emission inventory for the year 2004 and (b) spatial distribution of the SCIAMACHY tropospheric NO$_2$ vertical columns for the year 2004.

period. Scenarios E3 and E4 affect the NO$_x$ emission trend during 1997–2002 and 2000–2002 differently; scenario E3 moves the emission trend closer to the satellite trend during 1997–2000, but for the whole period the change is relatively small and cannot be the dominant factor in the disagreement between inventories and satellite columns.

[57] 3. Changing emission factors have a significant impact on the emission trend. If we assume that NO$_x$ emission factors in coal-fired power plants remained constant at 8.9 g/kg over the entire period (F1), NO$_x$ emissions would have increased by 72% between 1996 and 2004, approaching the satellite trend. This warns us that the average NO$_x$ emission rate of power plants might not have improved as much as is generally believed during the past 10 a. A systematic study of typical power plant technology and operation by size of plant is necessary to reduce the uncertainty. When a constant emission factor of 8 g/kg NO$_x$ is assumed for all industrial coal combustion equipment, the F2 scenario shows higher NO$_x$ emissions but a lower rate of increase compared with the BGE scenario, resulting in a

larger gap between the emission and satellite trends. This suggests that a composite emission factor for a whole sector can introduce significant errors in an emission inventory, especially for long-term trends. Holding NO$_x$ emission factors for vehicles constant at the level of the late 1990s results in an emissions increase of 65% during 1996–2004, also approaching the satellite trend; however, the decrease of vehicle emission factors has been confirmed by real-world measurements [*Chen et al.*, 2007; *Yao et al.*, 2007], suggesting that the F3 scenario may not reflect China's actual situation.

[58] 4. Even considering all known uncertainty factors for the inventory, the discrepancy between emission inventory and satellite columns still cannot be fully explained. According to the above analysis, the E3 and F1 scenarios will generate emission trends that are closest to the satellite trend. We therefore generated a final MAX scenario by merging E3 and F1 together, as shown in Figure 6. In the MAX scenario, NO$_x$ emissions increase by 72% between 1996 and 2004, following a similar curve to the satellite

Table 7. Key Assumptions of Alternative Emission Scenarios

Scenario	Summary of Scenario Assumption	Reference Scenario (BGE)
E1	uses coal consumption data in the national energy balance table of energy statistics	uses coal consumption data in the provincial energy balance table of energy statistics
E2	uses diesel consumption data in the provincial energy balance table of energy statistics	uses diesel consumption data in the national energy balance table of energy statistics
E3	assumes that the energy efficiency of coal-fired power plants improved gradually, like line C in Figure 1	uses coal consumption data from energy statistics for power plants
E4	industrial coal consumption for 2001–2002 is extrapolated using a basic linear function, like line F in Figure 1	uses coal consumption data from energy statistics for industry sector
F1	assumes the average NO$_x$ emission factor for power plants remained constant at 8.9 g/kg over the whole period	assumes the average NO$_x$ emission factor for power plants decreased from 8.9 g/kg to 7.4 g/kg over the period, due to applications of LNB technology
F2	uses the value of 8 g/kg factor for all industrial coal combustion equipment	uses different emission factors for different industrial coal combustion equipment
F3	assumes that vehicle emission factors remained at the level of the late 1990s throughout the period	assumes that vehicle emission factors decreased over the period because of implementation of vehicle emission standards

Table 8. Comparison of NO$_x$ Emissions in the ECC Region for Different Emission Scenarios

	BGE		E1		E2		E3		E4		F1		F2		F3		MAX		
	EM[a]	AIR[b]	EM	AIR	EM	AIR	EM	AIR	EM	AIR	EM	AIR	EM	AIR	EM	AIR	EM	AIR	Satellite: AIR
1996	5.3	5.6	5.3	5.9	5.2	5.0	5.3	4.9	5.3	5.6	5.4	6.4	6.1	4.6	5.3	5.6	5.1	5.6	N/A
1997	5.4	1.6	5.3	−0.2	5.3	1.6	5.5	3.9	5.4	1.6	5.5	2.0	6.2	1.4	5.4	1.6	5.4	4.3	4.2
1998	5.4	−0.8	5.3	−0.6	5.2	−1.7	5.5	−0.6	5.4	−0.8	5.5	0.2	6.2	−0.4	5.4	−0.8	5.6	0.4	0.4
1999	5.5	2.6	5.4	1.9	5.3	1.9	5.7	3.8	5.5	2.6	5.7	3.6	6.3	2.0	5.5	2.6	5.6	4.9	6.9
2000	5.7	2.9	5.5	2.0	5.4	3.2	5.9	3.5	5.7	2.9	5.9	4.1	6.4	1.9	5.7	3.0	5.9	4.8	7.9
2001	6.0	6.1	5.7	4.3	5.8	6.9	6.2	4.6	6.1	7.8	6.3	7.1	6.7	4.8	6.0	6.5	6.2	7.1	7.5
2002	6.6	9.4	6.3	9.3	6.3	9.0	6.8	9.9	6.6	9.0	7.0	10.3	7.3	8.3	6.6	10.2	6.6	10.4	11.7
2003	7.3	11.3	7.0	11.7	7.1	12.6	7.4	9.3	7.3	9.9	7.8	12.2	8.1	11.0	7.5	12.4	7.3	8.8	20.1[c]
2004	8.5	16.8	8.2	18.0	8.3	15.7	8.5	15.2	8.5	16.8	9.2	17.9	9.3	14.8	8.8	18.0	7.9	16.1	12.4
Average	–	6.2	–	5.8	–	6.1	–	6.2	–	6.2	–	7.1	–	5.5	–	6.6	9.2	7.1	8.9
1996–2004[d]	–	60.3	–	54.8	–	59.3	–	60.3	–	60.3	–	71.8	–	51.8	–	65.4		71.8	95.5

[a]EM, emissions (Tg).
[b]AIR, annual increase rate (%).
[c]January and February data from GOME; after March 2003, data from SCIAMACHY.
[d]Total increase rate (%) from 1996 to 2004.

trends but still showing significant discrepancy. Further investigations of both inventory and satellite approaches are necessary to explain the remaining discrepancy.

4.6. Seasonal Variations in the Inventory and Satellite Data

[59] Figure 7a compares the monthly variation of NO$_x$ emissions in the inventory (BGE scenario) and the NO$_2$ vertical columns from GOME and SCIAMACHY for the ECC region from 1995 to 2004. The values have been normalized to January 1996, corresponding to the first available NO$_2$ vertical column data set from GOME. The two data sets have similar monthly profiles, both peaking in December. However, the winter peak of the satellite column data becomes sharper than the emission inventory data after the year 2000, causing the annual average NO$_2$ column to increase faster than the inventory.

[60] It should be noted that the lifetime of NO$_2$ also plays an important role in the seasonal variation of the NO$_2$

column. *Uno et al.* [2007] calculated NO$_2$ columns and NO$_2$ lifetimes over the ECC region using the CMAQ model. Both the CMAQ model and the GOME/SCIAMACHY results reproduced the summer minimum of the NO$_2$ column, which could not be found in the NO$_x$ emissions. Figure 7b presents the simulated monthly NO$_2$/NO$_x$ ratio

Figure 7. (a) Monthly variations in emission inventory and satellite observations over the ECC region. All data are normalized to January 1996. (b) Modeled atmospheric NO$_2$/NO$_x$ ratio under 1 km over the ECC region by the CMAQ model [adapted from *Uno et al.*, 2007].
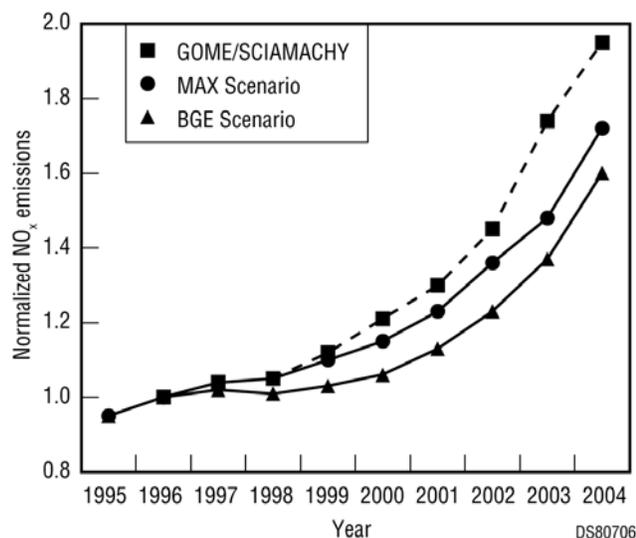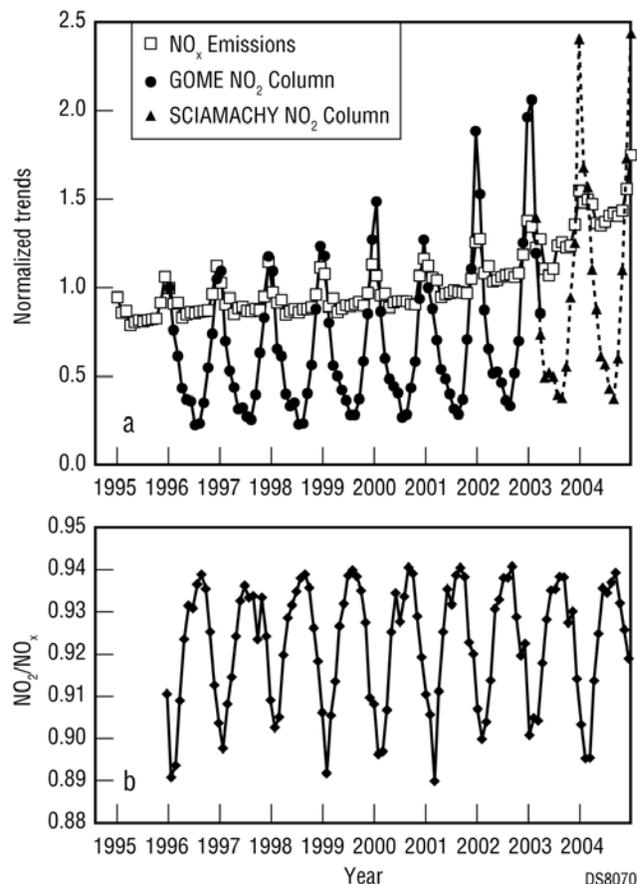

Figure 6. Temporal evolution of NO$_x$ emissions over the ECC region for the MAX scenario, in comparison to the BGE and satellite trends. All data are normalized to the year 1996.
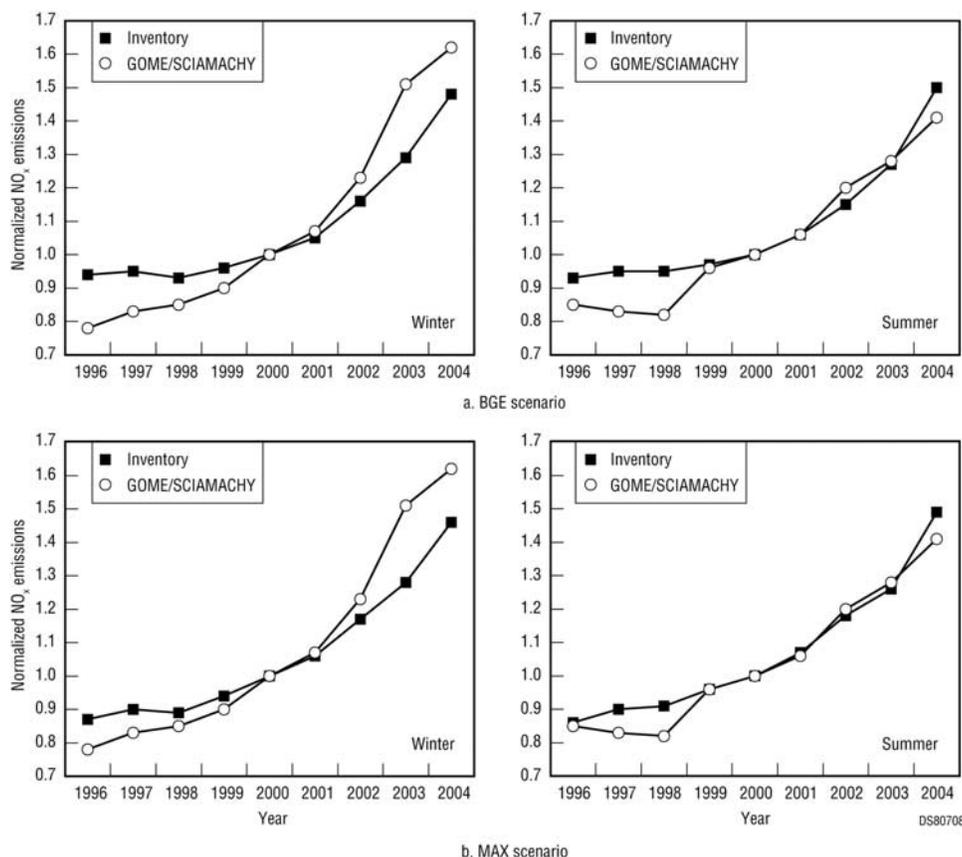
Figure 8. Temporal evolution of NO$_x$ emissions over the ECC region by inventory and satellite methods, by season, for the BGE and MAX scenarios. All data are normalized to the year 2000. Winter, November, December, January, and February; summer, May, June, July, and August.

below 1 km, clearly showing that the NO$_2$/NO$_x$ ratio has a maximum in summer and a minimum in winter. The NO$_2$/NO$_x$ ratio given by *Uno et al.* [2007] was calculated with an increased NO$_x$ emission trend from *Ohara et al.* [2007] (56% increase during 1996–2003), and NO$_2$ emissions assuming the ratio NO$_2$:NO = 1:9 from the emission sources. However, the NO$_2$/NO$_x$ ratio and NO$_2$ lifetime did not show a clear trend over the period.

[61] Figure 8a further compares the increasing trends of satellite columns and emissions by season under the BGE scenario. The two trends match well in summer. In the BGE scenario, summertime NO$_x$ emissions increase by 62% from 1996 to 2004, in good agreement with the 67% increase from the NO$_2$ satellite data. In winter, however, NO$_x$ emissions increase by 57%, while the NO$_2$ column data show an increase of 108%, about a factor of two greater. Identifying the reason for the wintertime discrepancy might be the key to explaining the disagreement between the inventory and the satellite retrievals.

5. Discussion
5.1. Possible Reasons for the Discrepancy

[62] We have used a dynamic methodology to represent China's NO$_x$ emission trends, assuming that emission factors change over time with changing technology. The uncertainty of emission factors will impact the accuracy of the NO$_x$ emission trends. Figure 8b compares the increasing

trends of satellite columns and emissions by season under the MAX scenario, which includes the sensitivity analysis. In the MAX scenario, NO$_x$ emissions in the ECC region increase by 68% in winter during the period 1996–2004, still presenting a discrepancy with the satellite trends. This suggests that uncertainty in annual activity rates and emission factors is not the key reason for the wintertime discrepancy. This conclusion is supported by the good agreement in summertime.

[63] It is conceivable that an increasing trend of emission factors in wintertime could cause the winter emission trends to be higher than expected. In this work, we did not consider any seasonal variation of emission factors. One possible explanation is that the NO$_x$ emission factor of power plants in winter increased after the year 2000. This might be associated with the coal shortage in China. Power plants are facing difficulties in obtaining sufficient coal in wintertime, when coal demand reaches its peak. Some plants may have been forced to burn lean coal in winter, which has a larger NO$_x$ emission factor than bituminous coal. However, this possibility cannot be verified with any official statistics.

[64] There are also reasons why satellite retrievals might be less reliable in wintertime. Inadequate treatment of satellite scenes with temporary snow cover could bias the observations. *Wang et al.* [2007] estimated this bias to be up to 20%. In winter, the Sun is lower during the satellite overpass, and therefore the measurement geometry is less

favorable for the measurement of tropospheric NO$_2$. Also, the lifetime of NO$_2$ is longer in winter, causing the link between emissions and the NO$_2$ column to be less direct, with pollutant transport and meteorology having a larger impact on the results. *Uno et al.* [2007] conducted a sensitivity study with fixed emissions for the year 2000. They found that a 10% difference in wind speed caused a 10% difference in NO$_2$ columns for fall and winter seasons, but that NO$_2$ columns are not strongly sensitive to the change of wind speed in spring and summer. The detection of emission trends over the ECC region from satellite data in fall or winter therefore resulted in larger errors because of the variability of meteorology.

[65] The injection height of the NO$_x$ emissions is also important. As the satellite measurements are less sensitive to NO$_2$ close to the ground, a trend at the surface will have less impact than a trend at 1 km altitude. This effect is more pronounced in winter than in summer, since the vertical profile sensitivity of the satellite measurements is a function of solar zenith angle at the time of satellite overpass. As the Sun is lower in winter than in summer for midlatitude measurements, the sensitivity to the surface layer is lower in winter than in summer. If this factor is taken in conjunction with the increasing emissions from large point sources with tall stacks, e.g., power plants and cement factories, it could be a factor in the larger winter trends viewed from space.

[66] One other plausible explanation from satellite retrievals is the changing trend of aerosol loading in China. The satellite retrievals assume there are no time trends in aerosol loading, which might not be appropriate for China. *Uno et al.* [2007] and *He et al.* [2007] found that China's SO$_2$ emissions increased by 30% from 2000 to 2003, which resulted in a 13% increase of sulfate in the ECC region. This will increase the aerosol single-scattering albedo. If this factor is not accounted for in the AMF calculation, it will introduce a trend in NO$_2$ columns even if NO$_2$ emissions are constant. Increasing sulfate aerosol concentration does not automatically increase the NO$_2$ observed, however. For NO$_2$ below the aerosol layer, the impact is opposite. However, for NO$_x$ injected with or above the aerosols, the visibility for the satellite increases. So emissions from large point sources have a larger impact on the satellite data. Aerosol scattering also influences the photolysis rate of NO$_2$, J(NO$_2$), thereby affecting the NO$_2$-to-NO ratio. The impact would be larger in winter than in summer, since SO$_2$ emissions in China have a peak in winter due to heating requirements, and measured SO$_4^{2-}$ concentrations in winter are usually 40–60% higher than in summer in more northerly cities [*He et al.*, 2001; *Sun et al.*, 2004]. This suggests that increased sulfate could be one of the possible reasons for the large difference in winter. Further studies are necessary to better understand the relationship between aerosol trends and satellite-retrieved NO$_2$ columns.

5.2. Trends in Ground-Level NO$_x$ Concentrations

[67] It is informative to compare the interannual emission trends with trends in measured ground-level NO$_x$ concentrations in China. Figure 9 shows the trends in annual average NO$_x$/NO$_2$ concentrations measured in 75 cities in the ECC region [*Editorial Committee of China Environmental Yearbook*, 1997–2005]. (Note that in the year 2000 China

switched its regulations from NO$_x$ to NO$_2$; in 2000 some cities reported NO$_x$ concentrations, while other cities reported NO$_2$ concentrations, and therefore we do not show data for 2000). Annual average NO$_x$ concentrations increased by 9% from 1995 to 1999, which is quite consistent with the 9% increase of NO$_x$ emissions from the inventory during the same period and with the 12% increase of GOME NO$_2$ column data from 1996 to 1999. However, the ground-level concentration trend is dramatically different after the year 2000. Measured annual average NO$_2$ concentrations remained relatively stable from 2001 to 2004, while both the NO$_x$ emission inventory estimates and the NO$_2$ satellite column data show an increase of more than 40% for that period.

[68] Figure 9 further shows the spatial characteristics of both the emission and concentration trends. Figure 9a presents the ratio of regional NO$_x$ emissions in 1999 and 1995, while Figure 9b presents the ratios of annual average NO$_x$ concentrations in 75 Chinese cities in 1999 and 1995. Figures 9c and 9d present similar pictures for the period between 2001 and 2004. It can be seen that NO$_x$ emissions increased by more than 20% from 2001 to 2004 in almost all provinces in the ECC region, while NO$_2$ concentrations in many cities in that region kept constant or even decreased. These maps show large inconsistencies between ground-level concentrations and emission estimates/satellite columns between 2001 and 2004. We can shed light on this curious situation by decomposing the driving forces of NO$_x$ emission increases during that period.

[69] In the ECC region, emissions from power plants contributed 52% of the NO$_x$ emissions increase between 2001 and 2004, and emissions from diesel fuel contributed 25%. Emissions from power plants usually have a high release height, causing a relatively lower contribution to ground-level concentrations. For example, NO$_x$ emissions from power plants contributed 27% of total NO$_x$ emissions in Beijing, yet were estimated to contribute only 1.4% to Beijing average ground-level concentrations in the year 2000 [*Hao et al.*, 2007]. More of the NO$_x$ is dispersed and transported to higher levels of the troposphere, causing an increase in the NO$_2$ column at regional scale. Diesel fuel is widely used in farm machines, tractors, rural vehicles, locomotives, vessels, etc., which typically are not located within cities; and diesel trucks drive more mileage on intercity transport than on intracity transport. Thus urban areas, where the monitoring sites are typically located, are not affected so much by the increase of NO$_x$ emissions. We can conclude that the nature of NO$_x$ pollution in China is changing from an essentially urban problem to one of more regional nature that may not be reflected in the urban monitoring data.

6. Conclusions

[70] We use a dynamic methodology to present the dramatic increase in China's emissions in recent years, driven by energy growth and technology renewal. With this new methodology, we derive a 10-a regional trend of NO$_x$ emissions in China from 1995 to 2004 and compare the emission trends with NO$_2$ column trends observed from space. Our best estimates for China's NO$_x$ emissions are 10.9 Tg in 1995 and 18.6 Tg in 2004, increasing by 70%
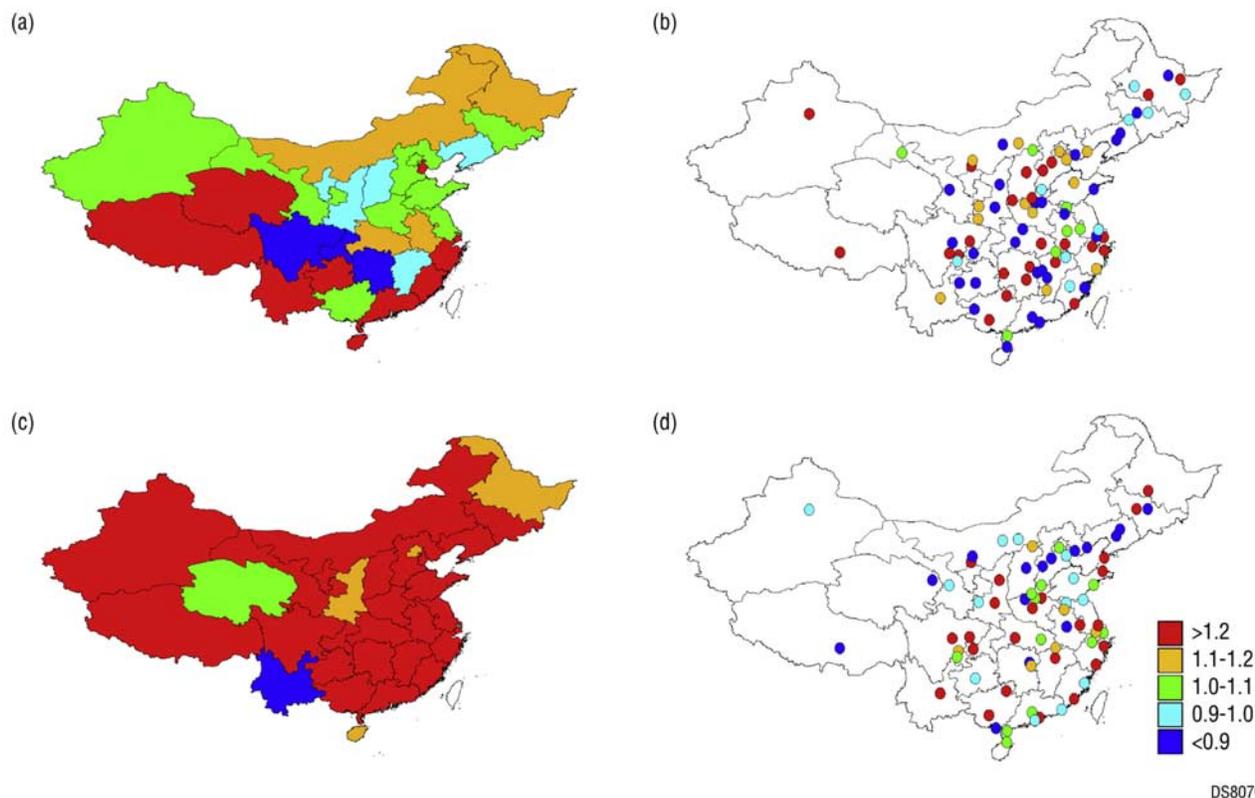
Figure 9. Changes in NO$_x$ emissions and measured NO$_x$ concentrations: (a) ratios of provincial NO$_x$ emissions in 1999 and 1995, (b) ratios of annual average NO$_x$ concentrations in 75 Chinese cities in 1999 and 1995, (c) ratios of provincial NO$_x$ emissions in 2004 and 2001, and (d) ratios of annual average NO$_2$ concentrations in 75 Chinese cities in 2004 and 2001.

during the period, with an accelerated growth rate. With the new methodology, we explore the nature of the driving forces of NO$_x$ emission growth over the period. The NO$_x$ emission increase before the year 2000 is largely attributed to increasing emissions from vehicles and the cement industry, while it is mainly driven by power plant emissions growth after 2000.

[71] Broad agreement was found between emission inventory and satellite observations. Both the emission inventory data and the satellite observations indicate a continuous and accelerating growth rate between 1996 and 2004 over the ECC region. However, the growth rate from the emission inventory is clearly lower than that from the satellite observations, even considering the system errors. From 1996 to 2004, NO$_x$ emissions over the ECC region increased by 61%, according to the inventory, while a 95% increase in the NO$_2$ columns measured by satellite was observed during the same period. Scenario-based sensitivity analysis indicates that the discrepancy cannot be fully explained by the uncertainty of the inventory.

[72] When comparing the NO$_x$ emission trends and the space-based NO$_2$ column trends by season, we found very good agreement during summertime but a large discrepancy during wintertime. The disagreement between the emissions and satellite column trends is confined to wintertime. The reasons for this discrepancy cannot be identified solely from the inventory perspective, as the consistency between summertime trends suggests that the bias cannot be associated with systematic error of the basic inventory data. Possible explanations include an underestimation of seasonal emission variations, variability of meteorology, NO$_x$ injection height, and the increasing trend of sulfate aerosols. Our study suggests that a joint analysis of the a priori inventory and the satellite-based observations would help to identify and reduce the uncertainties on both sides. A comprehensive forward/inverse modeling study driven by a state-of-the-art emission inventory would also be very beneficial. The recently launched OMI and GOME2 platform combines a relatively high spatial resolution with daily global coverage; it continues to record China's NO$_2$ trend. Continued improvement and update of the bottom-up inventory is required to follow the same track into the future.

References

Akimoto, H., and H. Narita (1994), Distribution of SO$_2$, NO$_x$ and CO$_2$ emissions from fuel combustion and industrial activities in Asia with 1° × 1° resolution, *Atmos. Environ.*, *28*, 213–225.

Akimoto, H., T. Ohara, J. Kurokawa, and N. Horii (2006), Verification of energy consumption in China during 1996–2003 by using satellite observational data, *Atmos. Environ.*, *40*, 7663–7667.

Bai, N. (1996), The emission inventory of CO_2, SO_2, and NO_x in China, in *The Atmospheric Ozone Variation and its Effect on the Climate and Environment in China* (in Chinese), edited by X. J. Zhou, pp. 145–150, Meteorological Press, Beijing.

Beijing Huatong Market Information Co. Ltd. (1996–2004), *China Latest Economic Indicators*, Beijing Huatong Market Inf., Beijing.

Beirle, S., U. Platt, M. Wenig, and T. Wagner (2003), Weekly cycle of NO_2 by GOME measurements: A signature of anthropogenic sources, *Atmos. Chem. Phys.*, 3, 2225–2232.

Benkovitz, C. M., M. T. Scholtz, J. Pacyna, L. Tarrason, J. Dignon, E. C. Voldner, P. A. Spiro, J. A. Logan, and T. E. Graedel (1996), Global gridded inventories for anthropogenic emissions of sulfur and nitrogen, *J. Geophys. Res.*, 101, 29,239–29,253.

Bey, I., et al. (2001), Global modeling of tropospheric chemistry with assimilated meteorology: Model description and evaluation, *J. Geophys. Res.*, 106, 23,073–23,096.

Bi, Y. (1998), Current situation, forecast and technical policy of NO_x emission of utility boilers (in Chinese), *China Power*, 31(12), 59–62.

Bovensman, H., et al. (1999), SCIAMACHY: Mission objectives and measurement modes, *J. Atmos. Sci.*, 56, 127–150.

Burrows, J. P., et al. (1999), The Global Ozone Monitoring Experiment (GOME): Mission concept and first scientific results, *J. Atmos. Sci.*, 56, 151–175.

Chen, C., et al. (2007), On-road emission characteristics of heavy-duty diesel vehicles in Shanghai, *Atmos. Environ.*, 41, 5334–5344.

China Association of Automobile Manufacturers (1991–2005), *China Automotive Industry Yearbook 1991–2005* (in Chinese), China Assoc. of Automobile Manuf., Beijing.

China Mechanical Industry Association (1996–2006), *China Mechanical Industry Yearbook 1995–2004* (in Chinese), China Mech. Ind. Express, Beijing.

China Petrochemical Corporation (2005), *China Petrochemical Corporation Yearbook 2005*, China Petrochem. Press, Beijing.

China Petroleum and Chemical Industry Association (2005), *China Chemical Industry Yearbook 2004–2005* (in Chinese), China Natl. Chem. Inf. Cent., Beijing.

China Statistical Information and Consultancy Center (1996–2004), *Monthly Bulletin of Statistics-China*, China Stat. Inf. and Consult. Cent., Beijing.

Chinese Research Academy of Environmental Sciences (2003), Description on developing emission standard of air pollutants for cement industry, internal report (in Chinese), Chinese Res. Acad. of Environ. Sci., Beijing.

Editorial Committee of China Environmental Yearbook (1997–2005), *China Environmental Yearbook*, China Environmental Science Press, Beijing.

Fisher-Vanden, K., G. H. Jefferson, H. Liu, and Q. Tao (2004), What is driving China's decline in energy intensity?, *Resour. Energ. Econ.*, 26, 77–97.

Fu, L., J. Hao, D. He, K. He, and P. Li (2001), Assessment of vehicular pollution in China, *J. Air Waste Manage. Assoc.*, 51, 658–668.

Hao, J., H. Tian, and Y. Lu (2002), Emission inventories of NO_x from commercial energy consumption in China, 1995–1998, *Environ. Sci. Technol.*, 36, 552–560.

Hao, J., L. Wang, M. Shen, L. Li, and J. Hu (2007), Air quality impacts of power plant emissions in Beijing, *Environ. Pollut.*, 147, 401–408.

He, K., F. Yang, Y. Ma, Q. Zhang, X. Yao, C. Chan, S. Cadle, T. Chan, and P. Mulawa (2001), The characteristics of $PM_{2.5}$ in Beijing, China, *Atmos. Environ.*, 35, 4959–4970.

He, K., H. Huo, and Q. Zhang (2002), Urban air pollution in China: Current status, characteristics, and progress, *Annu. Rev. Energy Environ.*, 27, 397–431.

He, K., H. Huo, Q. Zhang, D. He, F. An, M. Wang, and M. P. Walsh (2005), Oil consumption and CO_2 emissions in China's road transport: Current status, future trends, and policy implications, *Energy Policy*, 33, 1499–1507.

He, Y., I. Uno, Z. Wang, T. Ohara, A. Richter, and J. P. Burrows (2007), Variations of the increasing trend of tropospheric NO_2 over Central East China during the past decade, *Atmos. Environ.*, 41, 4865–4876.

Intergovernmental Panel on Climate Change (2001), *Climate Change 2001: The Scientific Basis: Contribution of Working Group I to the Third Assessment Report of the Intergovernmental Panel on Climate Change*, edited by J. T. Houghton et al., 881 pp., Cambridge Univ. Press, New York.

Irie, H., et al. (2005), Evaluation of long-term tropospheric NO_2 data obtained by GOME over East Asia in 1996–2002, *Geophys. Res. Lett.*, 32, L11810, doi:10.1029/2005GL022770.

Jaeglé, L., L. Steinberger, R. V. Martin, and K. Chance (2005), Global partitioning of NO_x sources using satellite observations: Relative roles of fossil fuel combustion, biomass burning and soil emissions, *Faraday Discuss.*, 130, 407–423.

Kato, N., and H. Akimoto (1992), Anthropogenic emissions of SO_2 and NO_x in Asia: Emission inventories, *Atmos. Environ.*, 26, 2997–3017.

Kean, A. J., R. F. Sawyer, and R. A. Harley (2000), A fuel-based assessment of off-road diesel engine emissions, *J. Air Waste Manage. Assoc.*, 50, 1929–1939.

Kim, S.-W., A. Heckel, S. A. McKeen, G. J. Frost, E.-Y. Hsie, M. K. Trainer, A. Richter, J. P. Burrows, S. E. Peckham, and G. A. Grell (2006), Satellite-observed U.S. power plant NO_x emission reductions and their impact on air quality, *Geophys. Res. Lett.*, 33, L22812, doi:10.1029/2006GL027749.

Klimont, Z., J. Cofala, W. Schopp, M. Amann, D. G. Streets, Y. Ichikawa, and S. Fujita (2001), Projections of SO_2, NO_x, NH_3 and VOC emissions in East Asia up to 2030, *Water Air Soil Pollut.*, 130, 193–198.

Li, Z. (2005), The overview of low NO_x combustion and denitrification technology for coal-fired power plants in China, paper presented at the 2nd U.S.-China NO_x and SO_2 Control Workshop, U.S. Dep. of Energy, Dalian, China.

Ma, J., A. Richter, J. P. Burrows, H. Nüß, and J. A. van Aardenne (2006), Comparison of model-simulated tropospheric NO_2 over China with GOME-satellite data, *Atmos. Environ.*, 40, 593–604.

Martin, R. V., D. J. Jacob, K. Chance, T. P. Kurosu, P. I. Palmer, and M. J. Evans (2003), Global inventory of nitrogen oxide emissions constrained by space-based observations of NO_2 columns, *J. Geophys. Res.*, 108(D17), 4537, doi:10.1029/2003JD003453.

Martin, R. V., C. E. Sioris, K. Chance, T. B. Ryerson, T. H. Bertram, P. J. Wooldridge, R. C. Cohen, J. A. Neuman, A. Swanson, and F. M. Flocke (2006), Evaluation of space-based constraints on global nitrogen oxide emissions with regional aircraft measurements over and downwind of eastern North America, *J. Geophys. Res.*, 111, D15308, doi:10.1029/2005JD006680.

National Bureau of Statistics of China (1998), *China Energy Statistical Yearbook 1991–1996*, China Stat. Press, Beijing.

National Bureau of Statistics of China (2001), *China Energy Statistical Yearbook 1997–1999*, China Stat. Press, Beijing.

National Bureau of Statistics of China (2004), *China Energy Statistical Yearbook 2000–2002*, China Stat. Press, Beijing.

National Bureau of Statistics of China (2005), *China Energy Statistical Yearbook 2003*, China Stat. Press, Beijing.

National Bureau of Statistics of China (2006), *China Energy Statistical Yearbook 2004*, China Stat. Press, Beijing.

National Bureau of Statistics of China (1996–2005), *China Statistical Yearbook 1995–2004*, China Stat. Press, Beijing.

Ohara, T., H. Akimoto, J. Kurokawa, N. Horii, K. Yamaji, X. Yan, and T. Hayasaka (2007), An Asian emission inventory of anthropogenic emission sources for the period 1980–2020, *Atmos. Chem. Phys. Disc.*, 7, 6843–6902.

Olivier, J. G. J., A. F. Bouwman, C. W. M. van der Maas, J. J. M. Berdowski, C. Veldt, J. P. J. Bloos, A. J. H. Visschedijk, P. Y. J. Zandveld, and J. L. Haverlag (1996), Description of EDGAR version 2.0, *Rep. 771060 002*, Natl. Inst. of Public Health and the Environ., Bilthoven, Netherlands.

Olivier, J. G. J., A. F. Bouwman, K. W. van der Hoek, and J. J. M. Berdowski (1998), Global air emission inventories for anthropogenic sources of NO_x, NH_3 and N_2O in 1990, *Environ. Pollut.*, 102, 135–148.

Olivier, J. G. J., J. P. J. Bloos, J. J. M. Berdowski, A. J. H. Visschedijk, and A. F. Bouwman (1999), A 1990 global emission inventory of anthropogenic sources of carbon monoxide on $1° \times 1°$ developed in the framework of EDGAR/GEIA, *Chemosphere*, 1, 1–17.

Olivier, J. G. J., J. A. van Aardenne, F. Dentener, V. Pagliari, L. N. Ganzeveld, and J. A. H. W. Peters (2005), Recent trends in global greenhouse gas emissions: Regional trends 1970–2000 and spatial distribution of key sources in 2000, *Environ. Sci.*, 2, 81–99.

Peking University (2001), Research on air pollution control strategy in Beijing (in Chinese), research report, Beijing.

Prather, M. J., et al. (2001), Atmospheric chemistry and greenhouse gases, in *Climate Change 2001: The Scientific Basis: Contribution of Working Group I to the Third Assessment Report of the Intergovernmental Panel on Climate Change*, edited by J. T. Houghton et al., pp. 239–287, Cambridge Univ. Press, New York.

Richter, A., J. P. Burrows, H. Nüß, C. Granier, and U. Niemeier (2005), Increase in tropospheric nitrogen dioxide levels over China observed from space, *Nature*, 437, 129–132.

Shah, J., et al. (2000), Integrated analysis for acid rain in Asia: Policy implications and results of RAINS-ASIA model, *Annu. Rev. Energy Environ.*, 25, 339–375.

Sinton, J. E. (2001), Accuracy and reliability of China's energy statistics, *China Econ. Rev.*, 12, 373–383.

Sinton, J. E., and D. G. Fridley (2000), What goes up: Recent trends in China's energy consumption, *Energy Policy*, 28, 671–687.

Sinton, J. E., K. R. Smith, and J. W. Peabody (2004), Programs to promote improved household stoves in China: An assessment of program performance, report to the Shell Found. Sustainable Energy Program, Inst. for Global Health, Univ. of Calif., San Francisco and Sch. of Public Health, Univ. of Calif., Berkeley.

State Environmental Protection Administration of China (1996), Emission standard of air pollutants for thermal power plants GB 13223–1996, State Environ, Prot. Admin., Beijing.

State Environmental Protection Administration of China (2003), Emission standard of air pollutants for thermal power plants GB 13223–2003, State Environ, Prot. Admin., Beijing.

Streets, D. G., and S. T. Waldhoff (2000), Present and future emissions of air pollutants in China: SO$_2$, NO$_x$, and CO, *Atmos. Environ.*, *34*, 363–374.

Streets, D. G., N. Y. Tsai, H. Akimoto, and K. Oka (2001), Trends in emissions of acidifying species in Asia, *Water Air Soil Pollut.*, *130*, 187–192.

Streets, D. G., et al. (2003), An inventory of gaseous and primary aerosol emissions in Asia in the year 2000, *J. Geophys. Res.*, *108*(D21), 8809, doi:10.1029/2002JD003093.

Streets, D. G., J. Hao, Y. Wu, J. Jiang, M. Chan, H. Tian, and X. Feng (2005), Anthropogenic mercury emissions in China, *Atmos. Environ.*, *39*, 7789–7806.

Streets, D. G., Q. Zhang, L. Wang, K. He, J. Hao, Y. Wu, Y. Tang, and G. R. Carmichael (2006), Revisiting China's CO emissions after TRACE-P: Synthesis of inventories, atmospheric modeling, and observations, *J. Geophys. Res.*, *111*, D14306, doi:10.1029/2006JD007118.

Su, D., D. Gao, and H. Ye (1998), Harmful gases pollution and its remedy in cement kiln (in Chinese), *Chongqing Environ. Sci.*, *20*(1), 20–23.

Sun, Y., G. Zhuang, Y. Wang, L. Han, J. Guo, M. Dan, W. Zhang, Z. Wang, and Z. Hao (2004), The air-borne particulate pollution in Beijing–Concentration, composition, distribution and sources, *Atmos. Environ.*, *38*, 5991–6004.

Tang, Q., X. Lu, S. Wang, and L. Zhou (1995), Industrial kiln gas pollution and its control (in Chinese), *Ind. Boiler*, *1995*(4), 42–47.

Tian, H. (2003), *Studies on Present and Future Emissions of Nitrogen Oxides and Its Comprehensive Control Policies in China*, Ph. D. thesis, Tsinghua Univ., Beijing.

Uno, I., et al. (2007), Systematic analysis of interannual and seasonal variations of model-simulated tropospheric NO$_2$ in Asia and comparison with GOME-satellite data, *Atmos. Chem. Phys.*, *7*, 1671–1681.

U.S. Environmental Protection Agency (1996), Compilation of air pollutant emission factors, *U.S. EPA Report AP-42*, U.S. Environ. Prot. Agency, Research Triangle Park, N. C.

Vallack, H., et al. (2001), Emission inventories for SO$_2$ and NO$_x$ in developing country regions in 1995 with projected emissions for 2025 according to two scenarios, *Water Air Soil Pollut.*, *130*, 217–222.

van Aardenne, J. A., G. R. Carmichael, H. Levy, D. Streets, and L. Hordijk (1999), Anthropogenic NO$_x$ emissions in Asia in the period 1990–2020, *Atmos. Environ.*, *33*, 633–646.

van der A, R. J., D. H. M. U. Peters, H. Eskes, K. F. Boersma, M. Van Roozendael, I. De Smedt, and H. M. Kelder (2006), Detection of the trend and seasonal variation in tropospheric NO$_2$ over China, *J. Geophys. Res.*, *111*, D12317, doi:10.1029/2005JD006594.

van Noije, T. P. C., et al. (2006), Multi-model ensemble simulations of tropospheric NO$_2$ compared with GOME retrievals for the year 2000, *Atmos. Chem. Phys.*, *6*, 2943–2979.

Wang, W., W. Wang, W. Zhang, and S. Hong (1996), Geographical distribution of SO$_2$ and NO$_x$ emission intensities and trends in China (in Chinese), *China Environ. Sci.*, *16*, 161–167.

Wang, Y. X., M. B. McElroy, T. Wang, and P. I. Palmer (2004), Asian emissions of CO and NO$_x$: Constraints from aircraft and Chinese station data, *J. Geophys. Res.*, *109*, D24304, doi:10.1029/2004JD005250.

Wang, Y. X., M. B. McElroy, R. V. Martin, D. G. Streets, Q. Zhang, and T.-M. Fu (2007), Seasonal variability of NO$_x$ emissions over east China constrained by satellite observations: Implications for combustion and microbial sources, *J. Geophys. Res.*, *112*, D06301, doi:10.1029/2006JD007538.

Woo, J.-H., J. M. Baek, J.-W. Kim, G. R. Carmichael, N. Thongboonchoo, S. T. Kim, and J. H. An (2003), Development of a multi-resolution emission inventory and its impact on sulfur distribution for Northeast Asia, *Water Air Soil Pollut.*, *148*, 259–278.

Xue, X., et al. (2003), China's action of closing-down the small thermal power generation units (STPGU) (in Chinese), *China Energy*, *3*, 9–12.

Xue, Z., Z. Yang, and X. Zhao (1999), Distribution of SO$_2$, NO$_x$ emissions in China, 1995, in *Proceedings of the Sixth International Conference on Atmospheric Science and its Applications to Air Quality*, pp. 132–140, China Ocean Press, Beijing.

Yan, C. (1997), *China Energy Development Report* (in Chinese), Economic Manage. Press, Beijing.

Yang, X. (2001), Analysis and forecast of China's gasoline, kerosene and diesel fuel market (in Chinese), *Petrol. Petrochem. Today*, *9*, 13–18.

Yao, Z., Q. Wang, K. He, H. Huo, Y. Ma, and Q. Zhang (2007), Characteristics of real world vehicular emissions in Chinese cities, *J. Air Waste Manage. Assoc.*, *57*, 1379–1386.

Zhang, H., J. Li, X. Xu, R. Zeng, and G. Yue (2005), NO$_x$ emission and its control in utility coal-fired boilers in China (in Chinese), *Chin. J. Power Eng.*, *25*, 125–130.

Zhang, J., et al. (2000), Greenhouse gases and other airborne pollutants from household stoves in China: A database for emission factors, *Atmos. Environ.*, *34*, 4537–4549.

Zhang, Z. X. (2003), Why did the energy intensity fall in China's industrial sector in the 1990s? The relative importance of structural change and intensity change, *Energ. Econ.*, *25*, 625–638.

Zhou, D., Y. Dai, and C. Yu (2003), *China's Sustainable Energy Scenarios 2020* (in Chinese), China Environ. Sci. Express., Beijing.

————————————

J. P. Burrows and A. Richter, Institute of Environmental Physics, University of Bremen, D-28359 Bremen, Germany.

D. Chen, K. He, Y. Lei, and Z. Yao, Department of Environmental Science and Engineering, Tsinghua University, Beijing 100084, China.

C. J. Jang, Office of Air Quality Planning and Standards, U.S. Environmental Protection Agency, Research Triangle Park, NC 27711, USA.

D. G. Streets and Q. Zhang, Decision and Information Sciences Division, Argonne National Laboratory, Argonne, IL 60439, USA. (dstreets@anl.gov)

I. Uno, Research Institute for Applied Mechanics, Kyushu University, Fukuoka 816-8580, Japan.

Y. Wang, Division of Engineering and Applied Sciences, Harvard University, Cambridge, MA 02138, USA.